

Chiral Thermomechanical Metamaterials with Continuous Negative Thermal Expansion

By

Debajyoti Saha

B.Tech., West Bengal University of Technology, 2017

THESIS

Submitted as partial fulfilment of the requirements for the degree of Master of Science in Civil Engineering in the Graduate College of the University of Illinois at Chicago, 2019

Chicago, Illinois

Defense Committee:

Eduard Karpov, Chair and Advisor

Mathew Daly, Civil and Materials Engineering

Sara Kadkhodaei, Civil and Materials Engineering

Aleksandr Fridlynd, Gas Technology Institute

Acknowledgement

I would like to thank my advisor Dr. Eduard Karpov for his unwavering support and assistance. Without his guidance, it would be very difficult for me complete my thesis. I would like to thank every committee member for spending their valuable time and giving me such great inputs. I would also like to thank Gas Technology Institute for supporting us for this project. I would also like to thank my parents, who stood by me and supported me all the time. At last, thanks to my friends, who were total strangers to me just two years back; but they have stood by me no matter what. Thank you everyone for supporting me and believing in me.

Abstract

Though the negative thermal expansion materials are important and appealing in science and engineering application, the natural materials are very less effective and manifest poor performance than the metamaterials. Here, using chiral design and normal material, metamaterial structure has been achieved. From the derivation, it has been proven that the structure contracted or expanded with an acceleration. It has also been observed that, the contraction or expansion rate depends upon the geometry of the structure (node to length ratio, i.e., size ratio). For the design scenario, node is the metallic structure helps to attach different number of strips. It has also been observed that, the state parameters and the control parameters (i.e. Temperature) share simple relationship between them. The rotation angle is a function of (property of the bimetallic strip), L (length of the strip) and T (temperature). Also, the maximum working temperature depends on the design parameters. So, it would be a metamaterial system. To dimensionalize, all the system equations have been scaled with L . So, length alone will not be a parameter of design, node to length ratio size ratio will be.

Table of Content

Chapter 1: Introduction.....	1
Chapter 2: Chiral metamaterials.....	3
2.1: Chiral meta materials with square node.....	3
2.2: Chiral meta materials with circular node.....	16
2.3: Chiral meta materials with triangular node.....	27
Chapter 3: Summary and Conclusion.....	37
Chapter 4: Future Work.....	38
Chapter 5: References.....	39
Vita.....	43

List of Figures

Fig. 1: Part of whole structure with square node.....	3
Fig. 2: Bimetallic strip with different width and Young's modulus.....	4
Fig. 3: one strip with two square nodes.....	5
Fig. 4: Square node expanded.....	6
Fig. 5: ϵ_T vs T plot for square node.....	8
Fig. 6: α_T vs T plot for square node.....	9
Fig. 7: α'_T vs T plot for square node.....	10
Fig. 8: ϵ_T , α_T and α'_T vs T graph for size ratio, $h = 0.115$ for square node.....	11
Fig. 9: The contour map for square node.....	12
Fig. 10: Solution for critical angle value (θ_C).....	13
Fig. 11: Comparison between θ_0 and θ_C	14
Fig. 12: Part of whole structure with circular node.....	15
Fig. 13: Diagram of unit cell with circular node.....	16
Fig. 14: one strip with two nodes for circular node.....	17
Fig. 15: Circular node expanded.....	18
Fig. 16: ϵ_T vs T plot for circular node.....	20
Fig. 17: α_T vs T plot for circular node.....	21
Fig. 18: α'_T vs T plot for circular node.....	22
Fig. 19: ϵ_T , α_T and α'_T vs T graph for size ratio, $d = 0.115$ for circular node.....	23
Fig. 20: The contour map for circular node.....	24
Fig. 21: Part of whole structure with triangular node.....	26
Fig. 22: Deformed diagram of unit cell with triangular node.....	27
Fig. 23: one strip with two triangular nodes.....	28
Fig. 24: Triangular node expanded.....	28
Fig. 25: ϵ_T vs T plot for triangular node.....	31
Fig. 26: α_T vs T plot for triangular node.....	32
Fig. 27: α'_T vs T plot for triangular node.....	33
Fig. 28: ϵ_T , α_T and α'_T vs T graph for size ratio, $h = 0.115$ for triangular node.....	35
Fig. 29: The contour map for triangular node.....	36

1 Introduction

“Metamaterials” is a term that classifies modern engineered materials which can possess extreme properties and functionality which are not available in the mother material. Veselago in 1967 [1] proved theoretically that the materials, which showed both negative permeability and negative permittivity, could express a remote property known as refractive index. Later Pendry and Smith [2-4] proved this concept in their experimental studies and used this concept on advanced resolution imaging and wave guiding technology [5-9]. But the term “Metamaterials” was first used by R.M. Walser in 2001 [10]. The prefix “meta” is coming from Greek language which can be translated as “beyond, after”. It reflects the fact that the metamaterials can react to external forces in completely different way than the conventional materials do.

Just after the World War 2, the history of metamaterials had started with artificial dielectrics in microwave engineering [11]. The concept of negative refractive index had been seen in wave mechanics as well, when it tuned to have both negative bulk modulus and negative mass density. Those studies stated that the sound waves can be operated to serve interesting applications like, shielding and reflection of waves through these metamaterials [11-14].

But the field of mechanical metamaterials is very novel and emerging. The main focus of this field is to produce materials with unexpected properties. The success in the field of optics and acoustics, where the negative refractive index has been achieved by arranging unit cells, has guided the theory and application of mechanical metamaterials. So, when an unfamiliar new type of geometry of a unit cell or any components of the material provides an opportunity to manipulate the mechanical properties like, stress, strain, stiffness, deformation etc., it can easily be stated that the material is mechanical metamaterial. From different authors it is available that these unusual properties of metamaterials are the result of unfamiliar elastic properties, i.e., Poisson’s ratio, Young’s modulus, bulk modulus and shear modulus, of the material achieved by the unit cell engineering [15-16]. It can be stated that with right engineering design extreme properties can be achieved which are not available in the mother materials.

In 1985, Kolpakov described an example of framework with negative Poisson’s ratio [17], which means that the framework will expand laterally when longitudinal tensile forces are applied. Later in 1987, Lakes described polyform foam structure, which has this behavior [18-19]. Now this behavior is called

“auxetics”. It can be stated that this behavior is only the property of nonconvex microstructure [20]. For this reason, this property is being used in aerospace and marine application for their absorption and light weight properties [21]. Materials which can absorb more or have high damping efficiency, i.e., own negative stiffness, defined as metamaterials as well [22-23].

Bistability [24] may in some cases be expressed as a characteristic of negative stiffness. It can bring some new rare properties in the materials, such as, negative compressibility [25-28], where the properly designed structure will contract upon the application of tensile load and in the load direction.

Having these advanced properties in a designed material, the application of these could lead to all exciting revolution in materials field, which later can be applied to professional fields, such as, architecture, manufacturing industry, transportation etc. Likewise, the known studies for negative compressibility [25-28], where the material contracts for a tensile load with the load direction, have discovered that these structures have multiple degrees of freedom. Whereas, in recent studies by Karpov [29], some engineered materials will pull back and contracts if the tensile load reaches a certain level.

The subject of this thesis is to provide some theoretical input for thermal metamaterials, which can thermal conduction [30]. Throughout the derivation and theory, it has been proved that with proper engineering design, i.e., change of length and dimension of the nodes, the curvature and the surface area can be controlled.

2.1 Chiral Meta-materials with Square Nodes

The metamaterial behavior of the structure drawn in fig.1 has been described in this section. Through the derivation done in this section, it can be proved that the design can behave as thermal metamaterial [30].

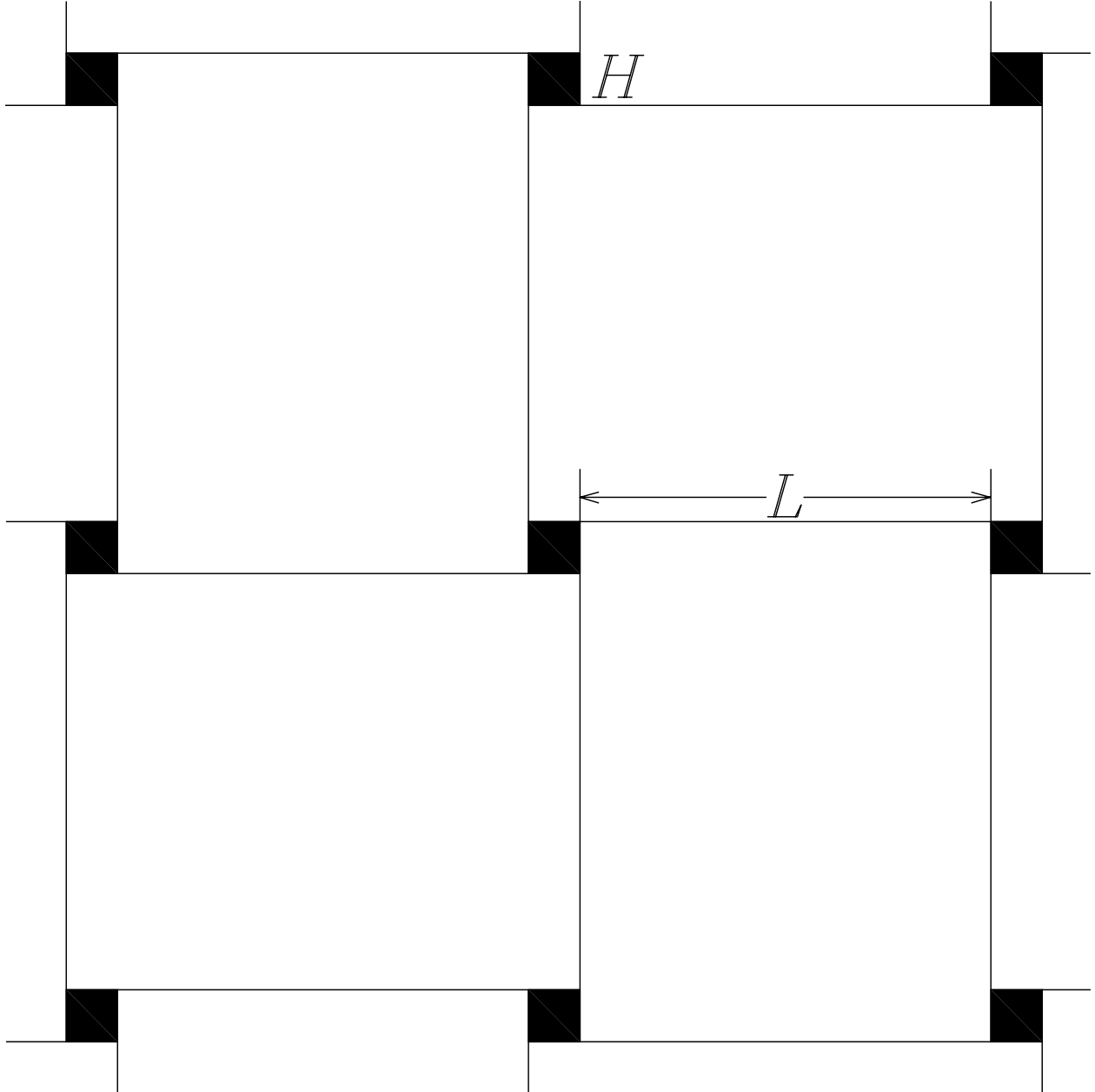


Fig. 1: Part of whole structure with square node



Fig. 2: Bimetallic strip with different width and Young's modulus

The curvature of the bimetallic beam κ can be represented as [31]:

$$\kappa = \frac{6E_1E_2(H_1+H_2)H_1H_2\varepsilon}{E_1^2H_1^4+4E_1E_2H_1^3H_2+6E_1E_2H_1^2H_2^2+4E_1E_2H_1H_2^3+E_2^2H_2^4} \quad (1)$$

or, $\kappa = a\varepsilon$

where, $a = \frac{6E_1E_2(H_1+H_2)H_1H_2}{E_1^2H_1^4+4E_1E_2H_1^3H_2+6E_1E_2H_1^2H_2^2+4E_1E_2H_1H_2^3+E_2^2H_2^4}$

E_1, E_2 = Young's modulus of two different sections,

H_1, H_2 = Width of two different sections.

If the dimension of the expression has been considered, it will be the dimension of inverse length and temperature. Expressed as:

$$[\kappa] = \frac{1}{[L][T]} \quad (2)$$

Where, $[L]$ = dimension of length, $[T]$ = dimension of temperature.

Again, the basic thermal strain expression of ε is [32]:

$$\varepsilon = \frac{l-l_0}{l_0} \quad (3)$$

Where, l = thermally expanded length, l_0 = original length.

Considering the geometry of the nodes as square and size of it as H and the length of the bimetallic strip as L , the equation has been formulated. Also, the thermal expansion coefficient of the strip denoted as α_s and the thermal coefficient of the node denoted as α_n .

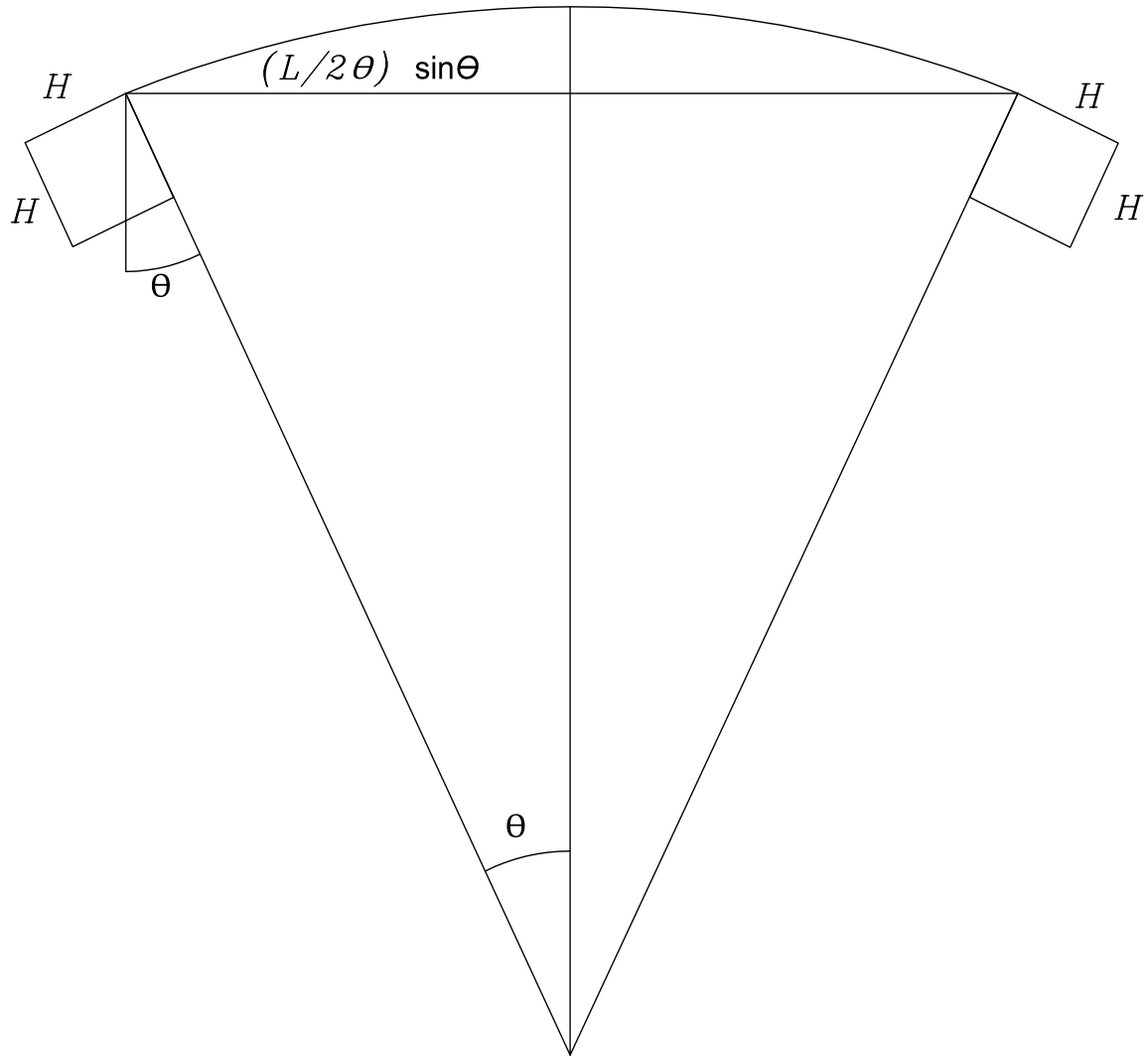


Fig. 3: one strip with two square nodes

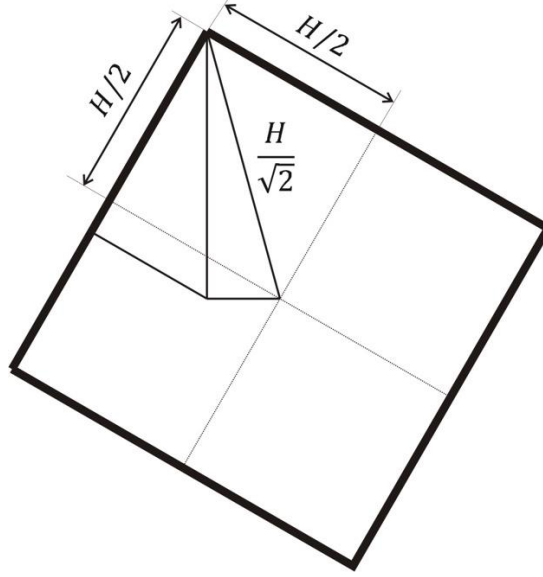


Fig. 4: Square node expanded

The deformed length of the strip depends on the curvature and the rate of thermal expansion. Using geometrical theories, the expression can be written as:

$$l = \frac{L_t}{\theta} \sin \theta + \sqrt{2} H_t \sin\left[\frac{\pi}{4} - \theta\right] \quad (4)$$

Where, l = deformed length between nodes, L_t = changed length of the strip after temperature has been applied, H_t = changed cross-sectional dimension after temperature has been applied, θ = radius of curvature.

In order to check the validity of the equation, the following condition can be made.

If $T=0$, there will not be any thermal expansion of the strips and nodes and any kind of curvature of the structure as well. So, θ will be zero as well. Now, from equation (4),

$$l = L + H \quad (5)$$

As temperature is not applied, the dimensions of the strips and the nodes will not be changed. That's why the notations L and H has been used instead of L_t and H_t in equation (5).

The basic expression for thermally expanded bar is [31]:

$$l_f = l_0 + l_0 \alpha \Delta T \quad (6)$$

Where, l_f = expanded final length, l_0 = initial length, α = thermal expansion coefficient and ΔT = temperature difference.

So, L_t and H_t can be written as using equation (6):

$$L_t = L(1 + \alpha_s T) \quad (7)$$

$$H_t = H(1 + \alpha_n T) \quad (8)$$

Now, replacing these two terms in equation (4) and rewriting the simplified form of it:

$$l = H(1 + \alpha_n T) \cos \theta + \frac{L(1 + \alpha_s T) - H(1 + \alpha_n T)\theta}{\theta} \sin \theta \quad (9)$$

Now this equation has dimension. For further analysis and plotting, it should be dimensionless. To non-dimensionalize the system, divide equation (9) by L . So, the dimensionless deformed length between two nodes will be:

$$l(\theta) = h(1 + \alpha_n T) \cos \theta + \frac{1 + \alpha_s T - \theta h(1 + \alpha_n T)}{\theta} \sin \theta \quad (10)$$

Where, size ratio, $h = \frac{H}{L}$.

The thermal strain of the system will be:

$$\epsilon_T = \frac{l(\theta, T)}{1 + h} - 1 \quad (11)$$

The simplified equation will be:

$$\epsilon_T = -1 + \frac{h(1 + \alpha_n T) \cos \theta + \frac{(1 + \alpha_s T - h(1 + \alpha_n T)\theta) \sin \theta}{\theta}}{1 + h} \quad (12)$$

The plot of ϵ_T vs T would be in fig. 5,

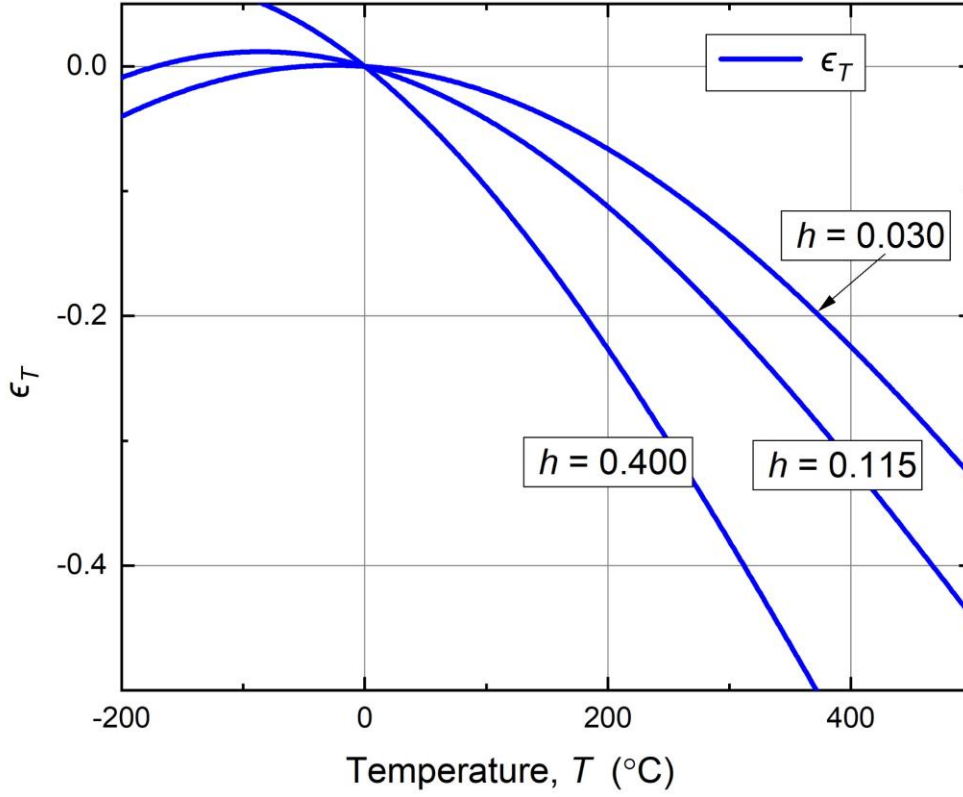


Fig. 5: Using equation (12), thermal strain (ϵ_T) vs temperature (T) has been plotted for three different size ratios ($h = \frac{H}{L}$)

The slope of thermal expansion curve, i.e., the thermal expansion co-efficient is:

$$\alpha_T = \frac{\theta(1+T\alpha_s-h(t\alpha_n(-1+\theta)+\theta))\cos\theta-(1+h\theta(\theta+T\alpha_n(1+\theta)))\sin\theta}{(1+h)T\theta} \quad (13)$$

If $\alpha_s = 0$ and $\alpha_n = 0$, α_T will be:

$$\alpha_T = \frac{\theta(1-h\theta)\cos\theta-(1+h\theta^2)\sin\theta}{(1+h)T\theta} \quad (14)$$

$$\theta = \frac{L}{\rho} \quad (15)$$

$$\frac{1}{\rho} = aT \quad (16)$$

“ a ” is a parameter of the strip, which depends on the properties of the strip. The value of “ a ” has to be calculated depending on the bending it shows with the temperature. For this validation, we have used equation (15) & (16) and calculated the value of “ a ” for the bimetallic strip used. To validate the equation experimentally, 60° bending of the 6" strip at $\Delta T = 70^\circ\text{C}$ is assumed. For this assumption, the angle of rotation looks reasonable.

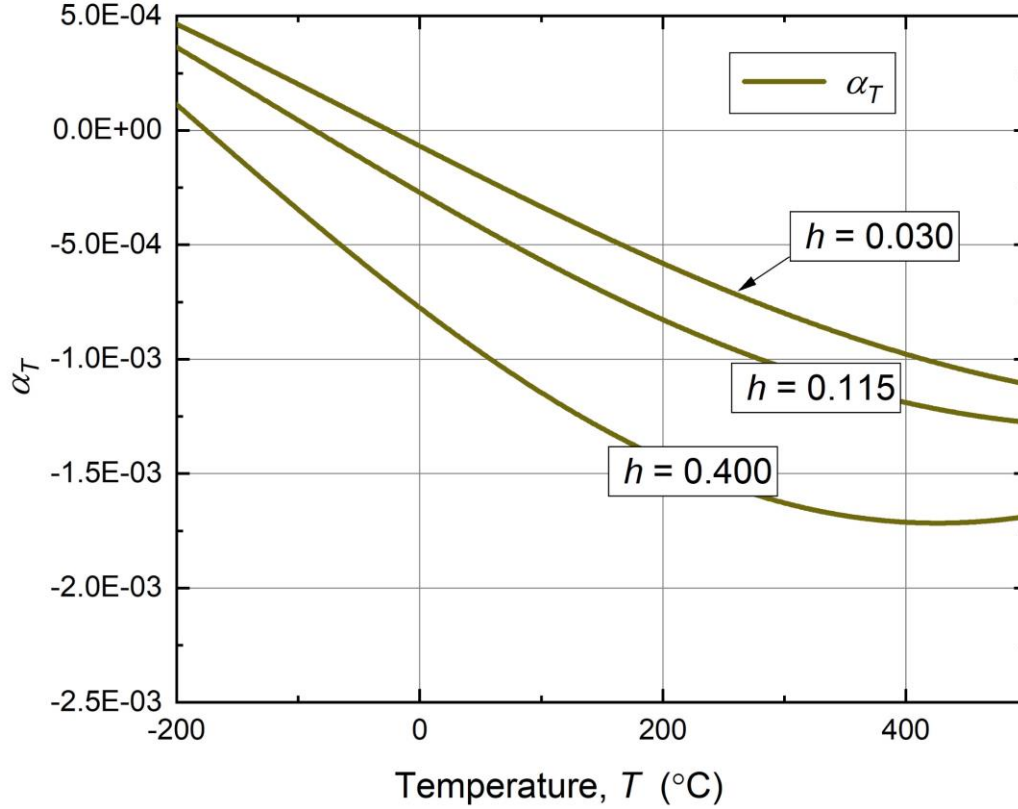


Fig. 6: Thermal expansion coefficient (α_T) vs temperature (T) plot using equation (13) for three different size ratios ($h = \frac{H}{L}$)

Now to know the acceleration of thermal expansion, the thermal strain ϵ should be derivated twice. So, it is as follows:

$$\alpha'_T = \frac{d\alpha}{dT} = \frac{d^2\epsilon}{dT^2} \quad (17)$$

Which can be expressed as:

$$\alpha'_T = \frac{1}{(1+h)T^2\theta} \left(-\theta \left(2 + h\theta(\theta + T\alpha_n(2 + \theta)) \right) \cos \theta + (2 - (1 + T(2h\alpha_n + \alpha_s))\theta^2 + (h + hT\alpha_n)\theta^3) \sin \theta \right) \quad (18)$$

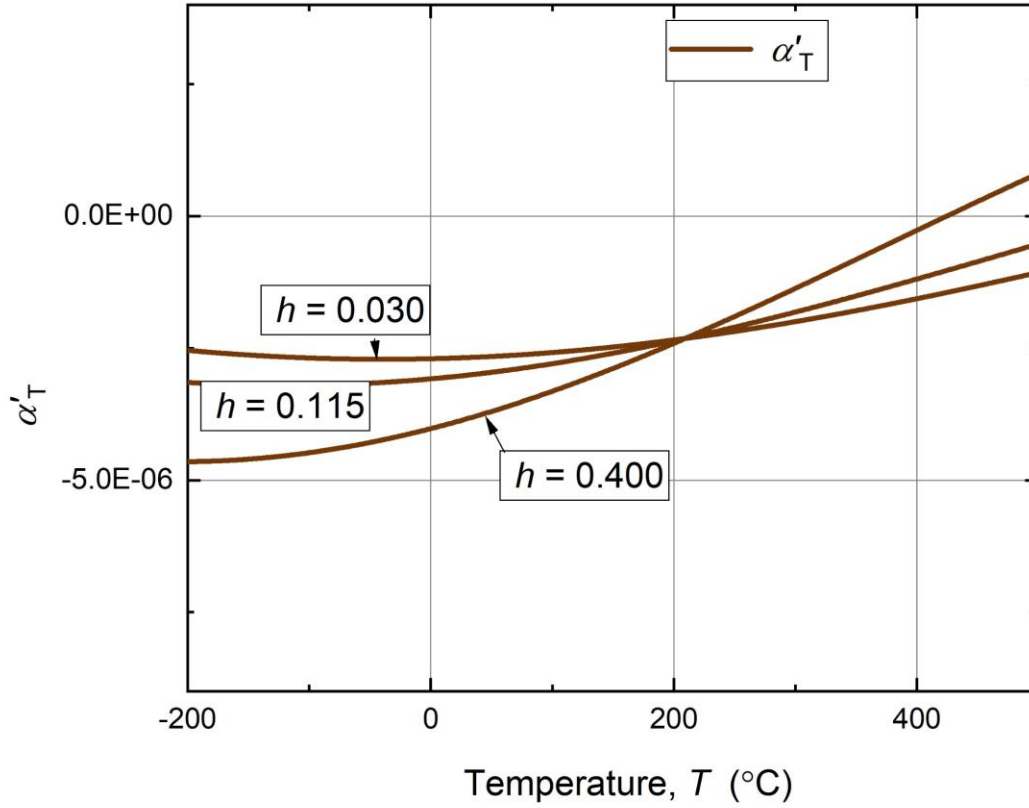


Fig. 7: Acceleration of thermal expansion coefficient (α'_T) vs temperature (T) plot using equation (18)

for three different size ratios ($h = \frac{H}{L}$)

Comparing the three parameters in a single plot in fig. 7 for the size factor of the design shown in the beginning of the chapter,

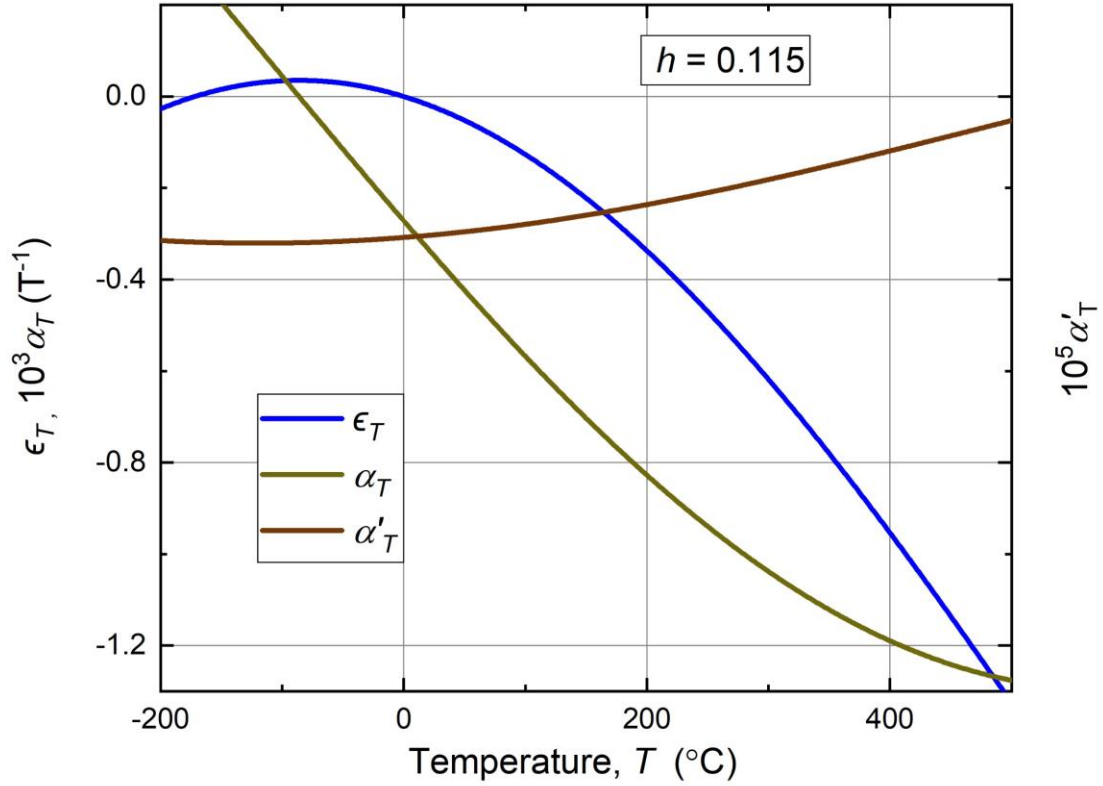


Fig. 8: For size ratio, $h = 0.115$, the three parameters are plotted together. To match the scale, with ϵ_T , α_T and α'_T has been multiplied by 10^3 and 10^5 respectively

$$\alpha'_0 = \lim_{T \rightarrow 0} \alpha'_T = -\frac{aL(aL+3aLh+12h\alpha_n)}{12(1+h)} \quad (19)$$

Where, θ has been replaced by $\theta = \frac{aLT}{2}$

Again,

$$\lim_{h \rightarrow 0} \alpha'_0 = -\frac{aL^2}{12}$$

And

$$\lim_{h \rightarrow \infty} \alpha'_0 = -\frac{1}{4}aL(aL + \alpha_n)$$

This curve proves that $\frac{d\alpha}{dT}$ at $T = 0$ is a monotonous function in spite of 3 parameters. So that it does not have any maximum in the range.

Considered $\alpha_s = \alpha_n$,

$$\alpha_0 = -\frac{aLh}{2(1+h)} + \alpha_s \quad (20)$$

If the points plotted in a contour plot, it would be:

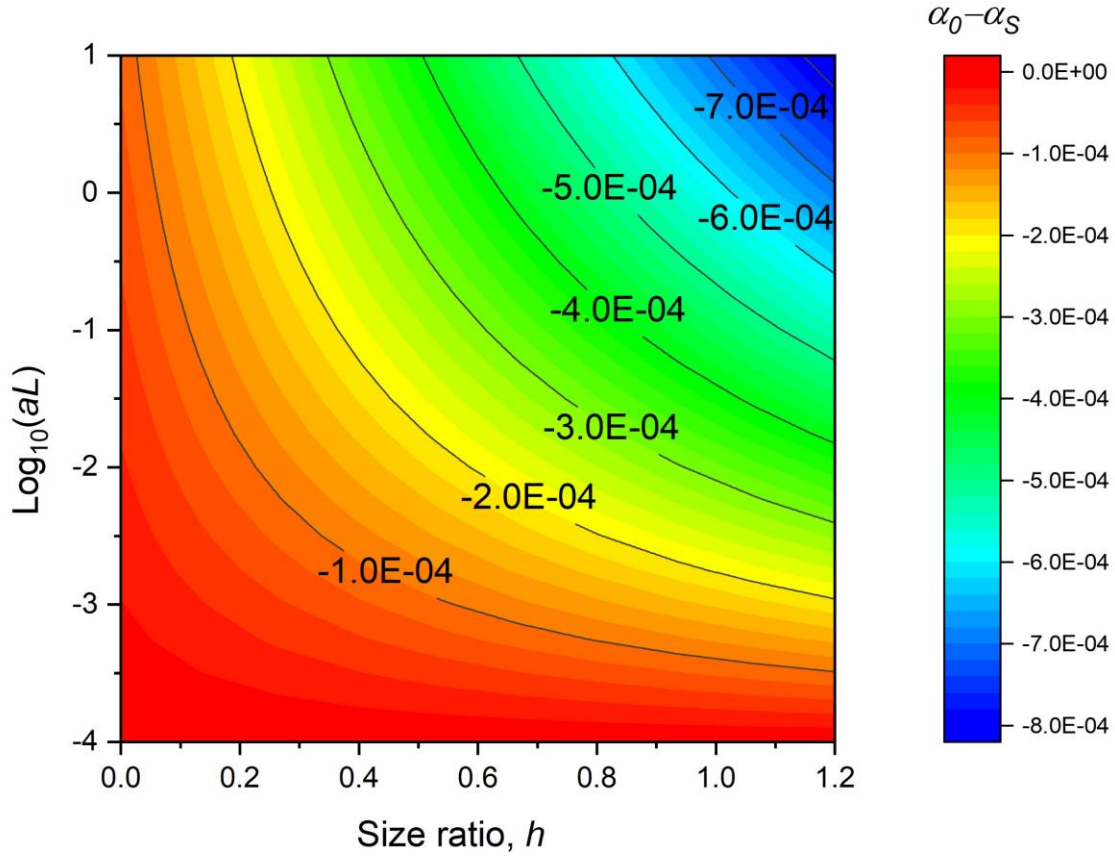


Fig. 9: The contour map has vertical axis as “ $\log_{10} aL$ ”, where “ aL ” have dimensionality of $[T]^{-1}$. As the dimension of “ a ” is $[L]^{-1}[T]^{-1}$ and “ L ” has dimension of $[L]$ (from equation (20)). So, it can be called as the rate of thermal expansion.

For this reason, it cannot be assumed that α_n doesn't have any effect on the system. For this system it is assumed that α_n has a little effect on it and this is also very much practically relatable as well. So, in mathematical terms, $\alpha_n \rightarrow 0$.

So, it can be written as in equation (19):

$$\alpha_0 = -\frac{aL(aL+3aLh)}{12(1+h)} \quad (21)$$

For the critical angle (i.e., when two opposite strips touch each other, the angle of rotation at that position) of the system, an assumption can be made, because before the strips will bend 90°, they will touch each other. Even this situation is theoretical. For the strips have been used in the model, it is quite impossible to achieve. So, the assumptions that has been made are:

- Horizontal deformed length= 2* Maximum possible vertical length (I_y)
- Natural thermal expansion is ignored

So, after simplification of the system equation using Mathematica, equation (20) has been achieved:

$$\tan \frac{\theta}{2} = 1 - 2h\theta \quad (22)$$

This equation actually has n-number of roots. So, the asymptotical solution of the system has been plotted with h in one axis.

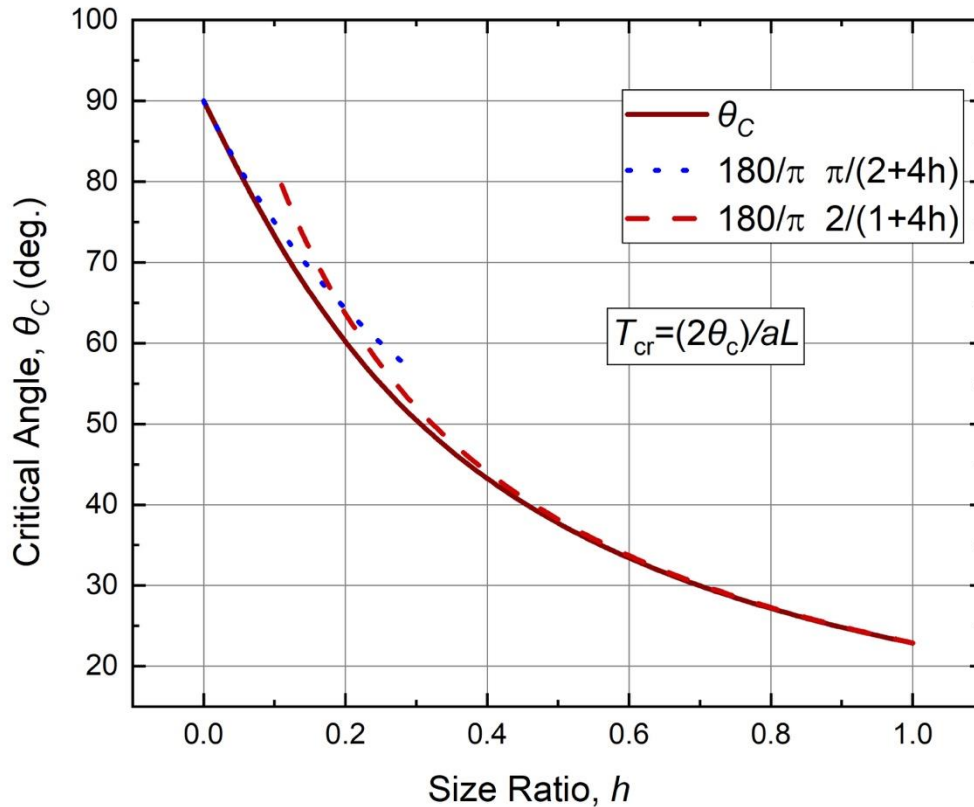


Fig. 10: Solution for critical angle value (θ_C). Asymptotic solution used equations (23) $\frac{180}{\pi} \frac{\pi}{2+4h}$ and (24)

$$\frac{180}{\pi} \frac{2}{1+4h}$$

Critical angle has been calculated with the formula used as:

$$\theta_c = \frac{aLT_c}{2} \quad (25)$$

Theoretically, α has a global minimum value. It can only be achievable at very high temperature. But it is not achievable for this type of design. Because, for high temperature, θ_0 will always be greater than θ_c , i.e., $\theta_0 > \theta_c$ for any given h . So, theoretically it is possible to achieve minimum value of α ; but practically it is not possible.

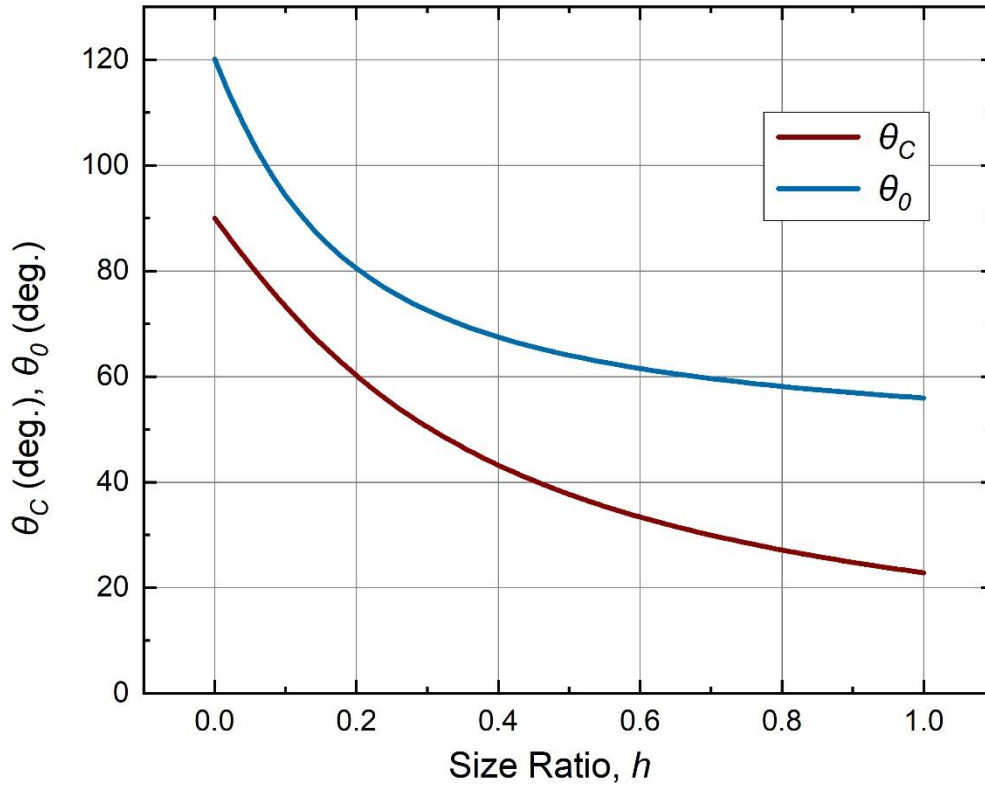


Fig. 11: Comparison between θ_0 and θ_c .

From the above theory and calculation, the system can achieve $\theta_c = 71.12^\circ$ and $T_c = 448.947^\circ\text{C}$.

2.2 Chiral Meta-materials with Circular Nodes

The metamaterial behavior of the structure drawn in fig.12 is described in this section. Through the derivation done in this section, it can be proved that the design can be worked as thermal metamaterial.

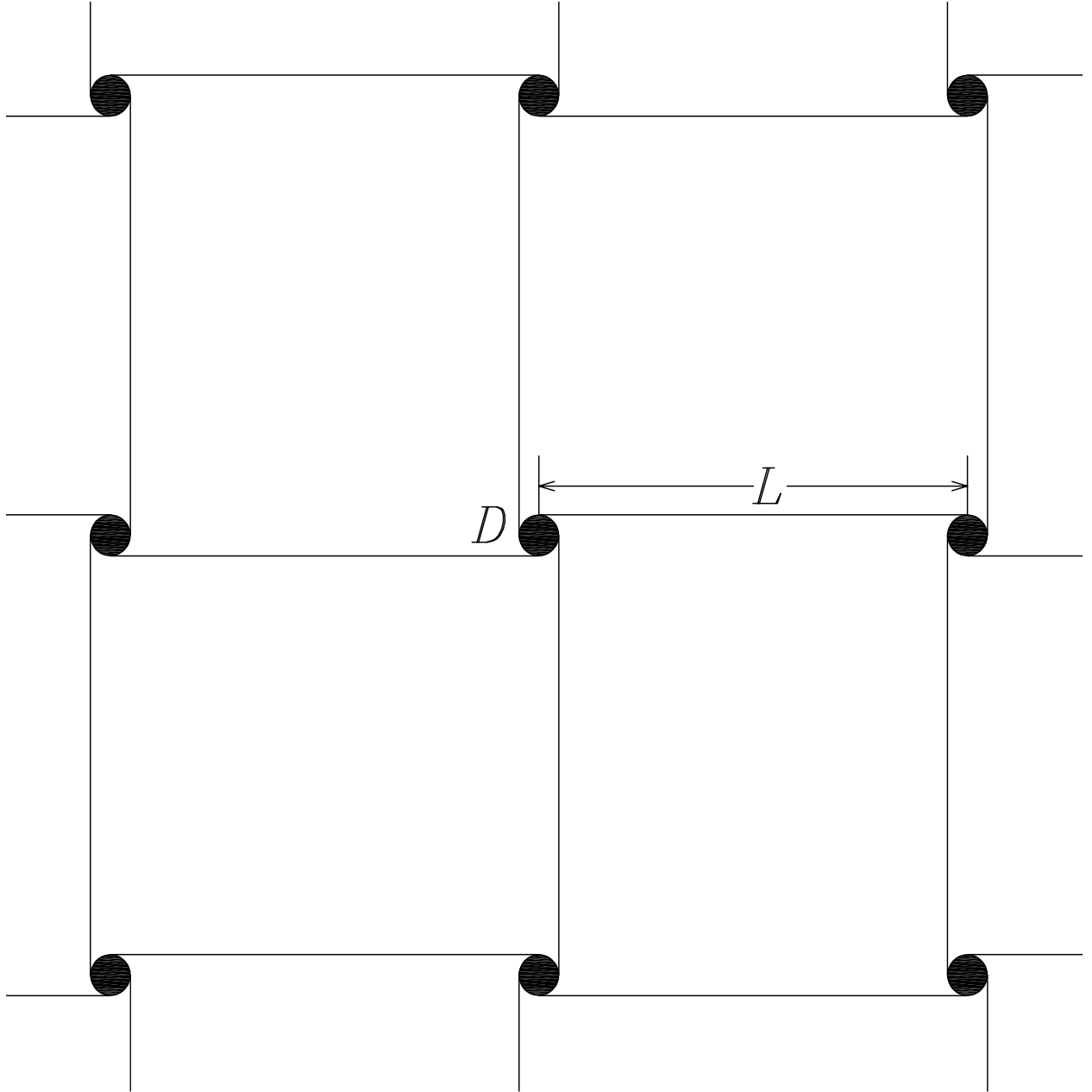


Fig. 12: Part of whole structure with circular node

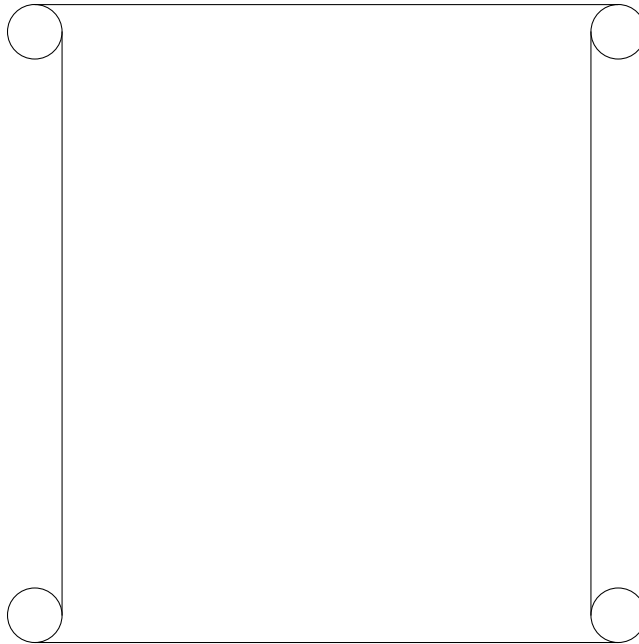


Fig. 13: Diagram of unit cell with circular node

Considering the geometry of the nodes as circular and diameter of the circle is D and the length of the bimetallic strip as L , the equation has been formulated. Also, the thermal expansion coefficient of the strip denoted as α_s and the thermal coefficient of the node denoted as α_n .

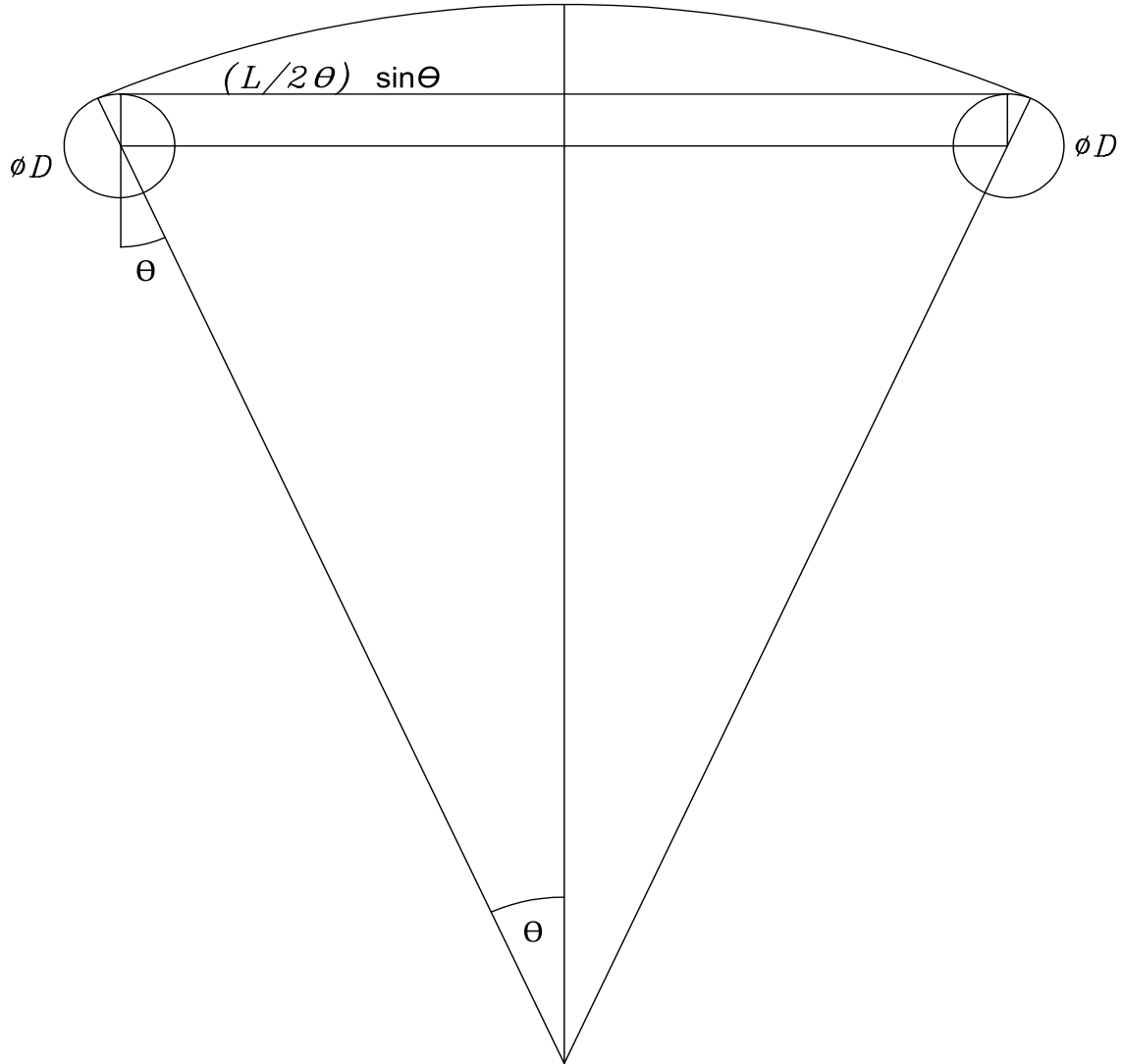


Fig. 14: one strip with two nodes

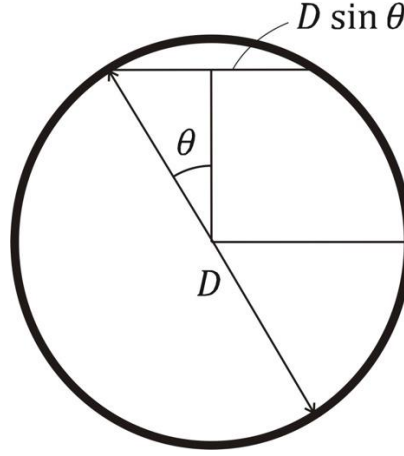


Fig. 15: Circular node expanded

The deformed length of the strip depends on the curvature and the rate of thermal expansion. Using geometrical theories, the expression can be written as:

$$l = \frac{L_t}{\theta} \sin[\theta] - D_n \sin[\theta] \quad (26)$$

Where, l = deformed length between nodes, L_t = changed length of the strip after temperature has applied, D_n = changed cross-sectional dimension after temperature has been applied, θ = radius of curvature.

In order to check the validity of the equation, the following condition can be made.

If $T=0$, there will not be any thermal expansion of the strips and nodes and any kind of curvature of the structure as well. Now, from equation (22),

$$l = L \quad (27)$$

As temperature is not applied, the dimensions of the strips and the nodes will not be changed.

That's why the notations L and D has been used instead of L_t and D_n .

The basic expression for thermally expanded bar is [31]:

$$l_f = l_0 + l_0 \alpha \Delta T \quad (6)$$

Where, l_f = expanded final length, l_0 = initial length, α = thermal expansion coefficient and ΔT = temperature difference.

So, L_t and D_n can be written as:

$$L_t = L(1 + \alpha_s T) \quad (7)$$

$$D_n = D_0(1 + \alpha_n T) \quad (8)$$

Now, replacing these two terms in equation (22) and rewriting the simplified form of it:

$$l(\theta) = \frac{(L(1+\alpha_s T) - D_0(1+\alpha_n T)\theta)\sin[\theta]}{\theta} \quad (28)$$

This equation has dimension. For further analysis and plotting, it should be dimensionless. To dimensionalize the system, divide by L . So, the dimensionless deformed length between two nodes will be:

$$l(\theta) = \frac{((1+\alpha_s T) - d(1+\alpha_n T)\theta)\sin[\theta]}{\theta} \quad (29)$$

Where, $d = \frac{D_0}{L}$.

The thermal strain of the system will be:

$$\epsilon_T = l(\theta, T) - 1 \quad (30)$$

The simplified equation will be:

$$\epsilon_T = -1 + \frac{(1+\alpha_s T - d(1+\alpha_n T)\theta)\sin[\theta]}{\theta} \quad (31)$$

The plot of ϵ_T vs T would be:

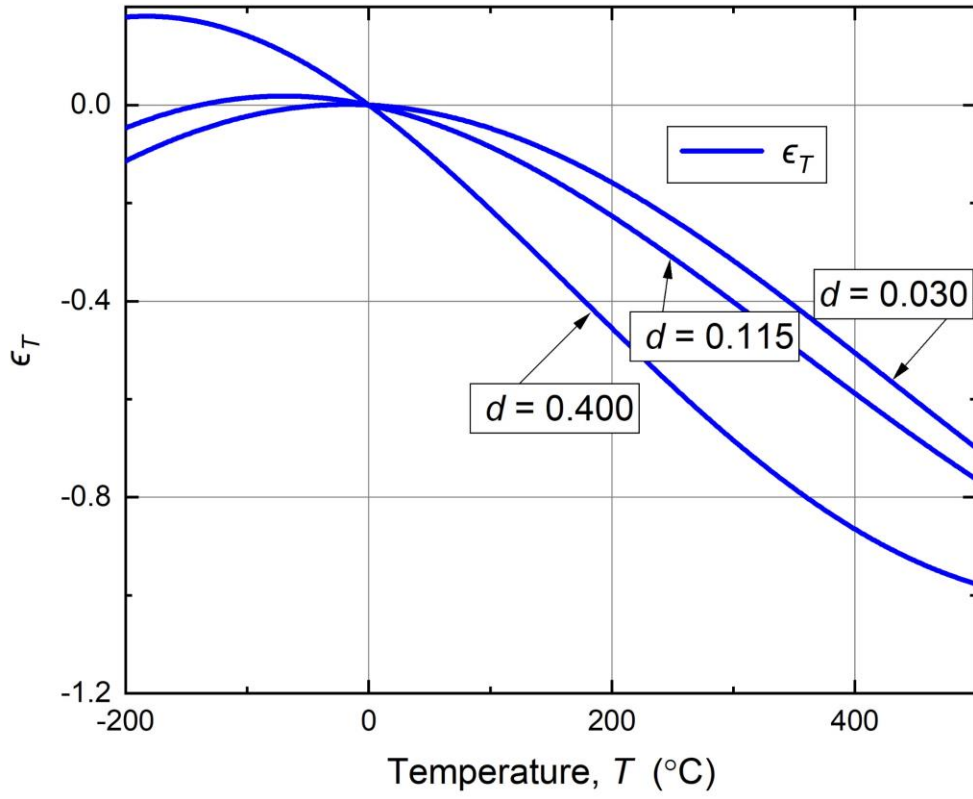


Fig. 16: Using equation (31), thermal strain (ϵ_T) vs temperature (T) has been plotted for three different size ratios ($d = \frac{D_0}{L}$)

The slope of thermal expansion curve, i.e., the thermal expansion co-efficient is:

$$\alpha_T = - \frac{\theta(-1-T\alpha_s+\theta d+Td\alpha_n\theta)\text{Cos}[\theta]+(1+Td\alpha_n\theta)\text{Sin}[\theta]}{T\theta} \quad (32)$$

If $\alpha_s = 0$ and $\alpha_n = 0$, α_T will be:

$$\alpha_T = -\frac{\theta(-1+d\theta)\cos[\theta]+\sin[\theta]}{T\theta} \quad (33)$$

$$\theta = \frac{L}{\rho} \quad (15)$$

$$\frac{1}{\rho} = aT \quad (16)$$

“ a ” is a parameter of the strip, which depends on the properties of the strip. The value of “ a ” has to be calculated depending on the bending it shows with the temperature. For this validation, we have used equation (15) & (16) and calculated the value of “ a ” for the bimetallic strip used. To validate the equation experimentally, 60° bending of the 6" strip at $\Delta T = 70^\circ\text{C}$ is assumed. For this assumption, the angle of rotation looks reasonable.

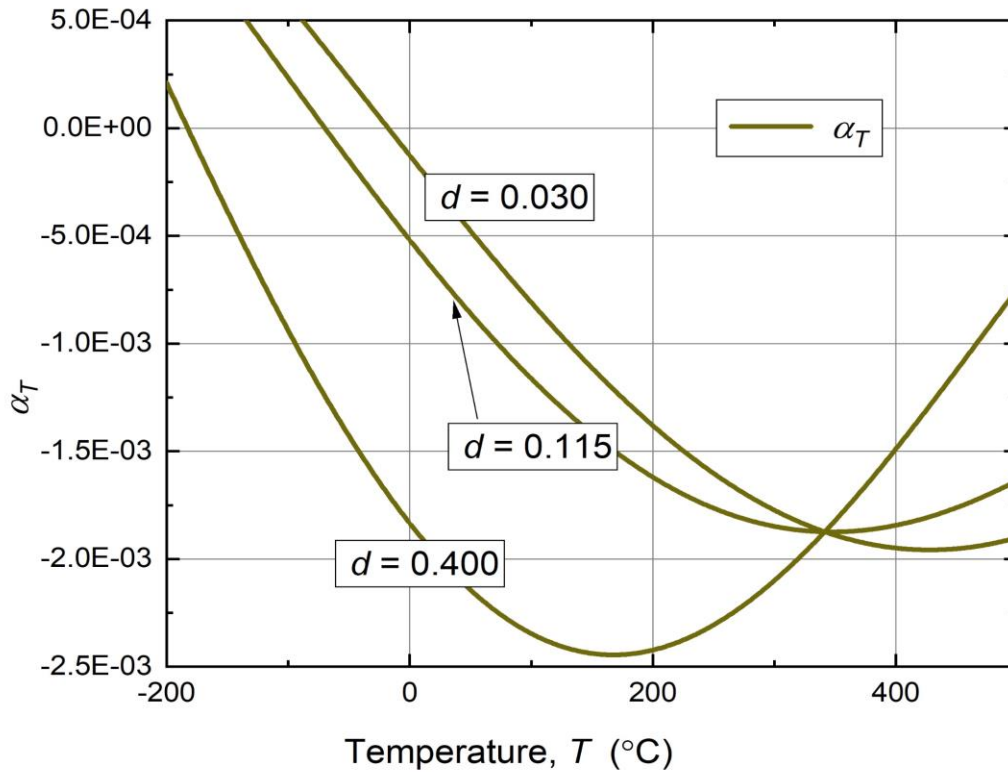


Fig. 17: Thermal expansion coefficient (α_T) vs temperature (T) plot using equation (32) for three different size ratios ($d = \frac{D_0}{L}$)

Now to know the acceleration of thermal expansion, the thermal strain ϵ should be derivated twice. So, it is as follows:

$$\alpha'_T = \frac{d\alpha}{dT} = \frac{d^2\epsilon}{dT^2} \quad (34)$$

Which can be expressed as:

$$\alpha'_T = \frac{-2\theta(1+dT\alpha_n\theta)\cos[\theta] + (2-(1+T\alpha_s)\theta^2 + (d+dT\alpha_n)\theta^3)\sin[\theta]}{T^2\theta} \quad (35)$$

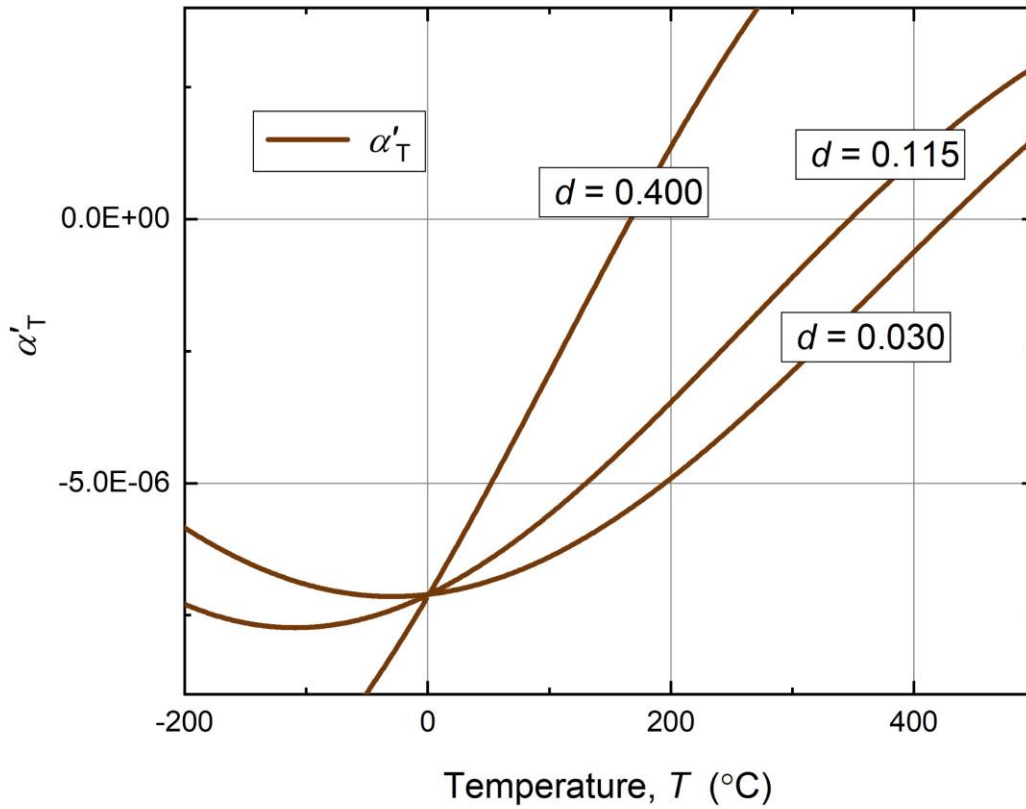


Fig. 18: Acceleration of thermal expansion coefficient (α'_T) vs temperature (T) plot using equation (35) for three different size ratios ($d = \frac{D_0}{L}$)

$$\alpha'_0 = \lim_{T \rightarrow 0} \alpha'_T = -\frac{1}{12} aL(aL + 12d\alpha_n) \quad (36)$$

Where, θ has been replaced by $\theta = \frac{aLT}{2}$

Again,
$$\lim_{d \rightarrow 0} \alpha_0 = -\frac{aL^2}{12}$$

And
$$\lim_{d \rightarrow \infty} \alpha_0 = aL\alpha_n(-\infty)$$

This curve proves that $\frac{d\alpha}{dT}$ at $T = 0$ is a monotonous function despite 3 parameters. So that it does not have any maximum in the range.

Comparing the three parameters in a single plot for the size factor of the design shown in the beginning of the chapter, it would look like:

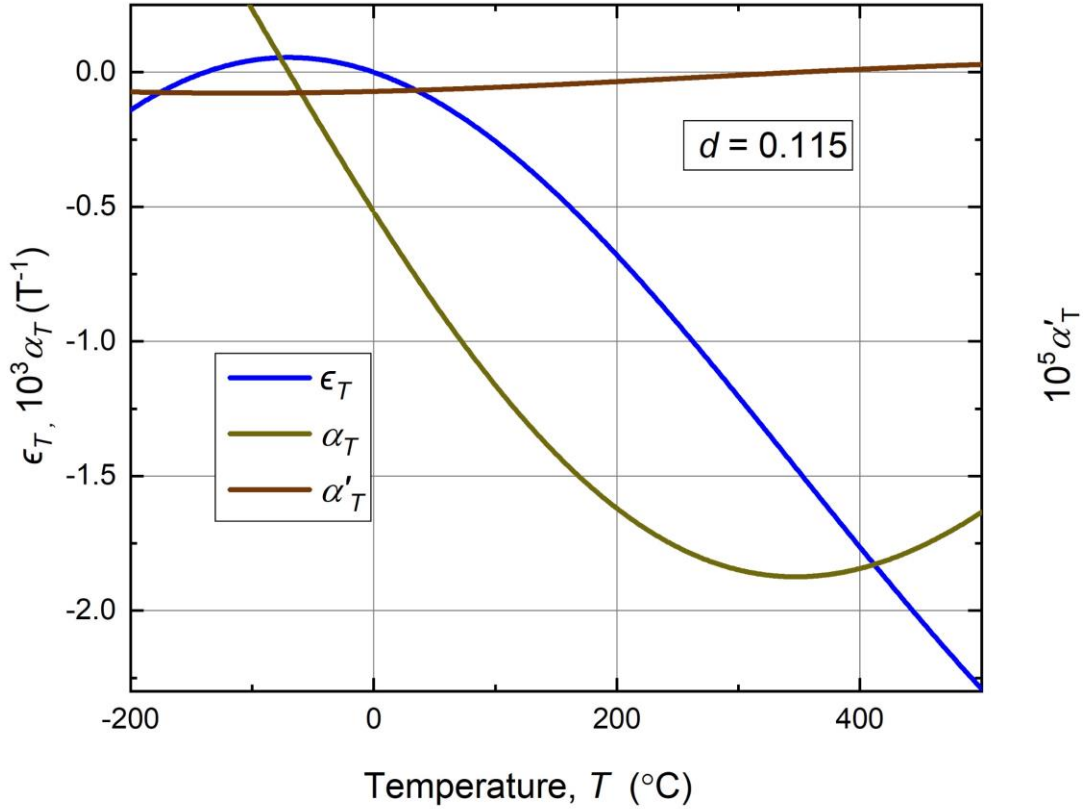


Fig. 19: For size ratio, $d = 0.115$, the three parameters are plotted together. To match the scale, with ϵ_T , α_T and α'_T has been multiplied by 10^3 and 10^5 respectively

To plot α_T and α'_T with ϵ_T , α_T and α'_T should be rescaled. Because these two have very small scale comparatively with ϵ_T . The previous individual graphs have been shown on the original scale.

Considered $\alpha_s = \alpha_n$,

$$\alpha_0 = -\frac{aLd}{2} + \alpha_s \quad (37)$$

If the points plotted in a contour plot, it would be as shown below:

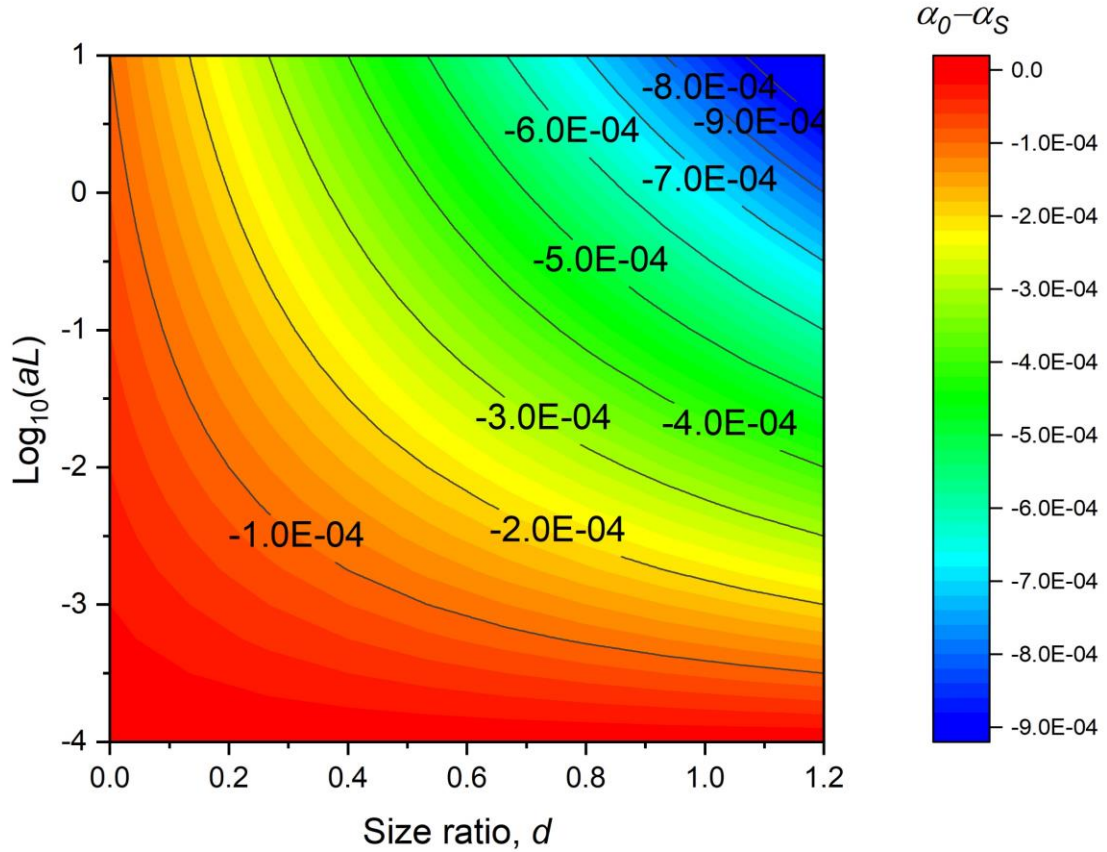


Fig. 20: The contour map has vertical axis as “ $\log_{10} aL$ ”, where “ aL ” have dimensionality of $[T]^{-1}$. As the dimension of “ a ” is $[L]^{-1}[T]^{-1}$ and “ L ” has dimension of $[L]$ (from equation (37)).

So, it can be called as the rate of thermal expansion.

For the circular nodes, the highest value of $\log_{10} aL = -9.8^{-4}$ in fig.19. Whereas in fig.8 for square node, this value comes down to $\log_{10} aL = -8.2^{-4}$. So, it easily can be stated that circular node is lot better than square node.

From the above theory and calculation, the system can achieve $\theta_c = 78.03^\circ$ and $T_c = 295^\circ\text{C}$. So, in simple words, it can reach higher critical angle with comparatively lower critical temperature.

2.3 Chiral Meta-materials with Triangular Nodes

The metamaterial behavior of the structure drawn in fig.21 has been described in this section. Through the derivation done in this section, it can be proved that the design can be worked as thermal metamaterial.

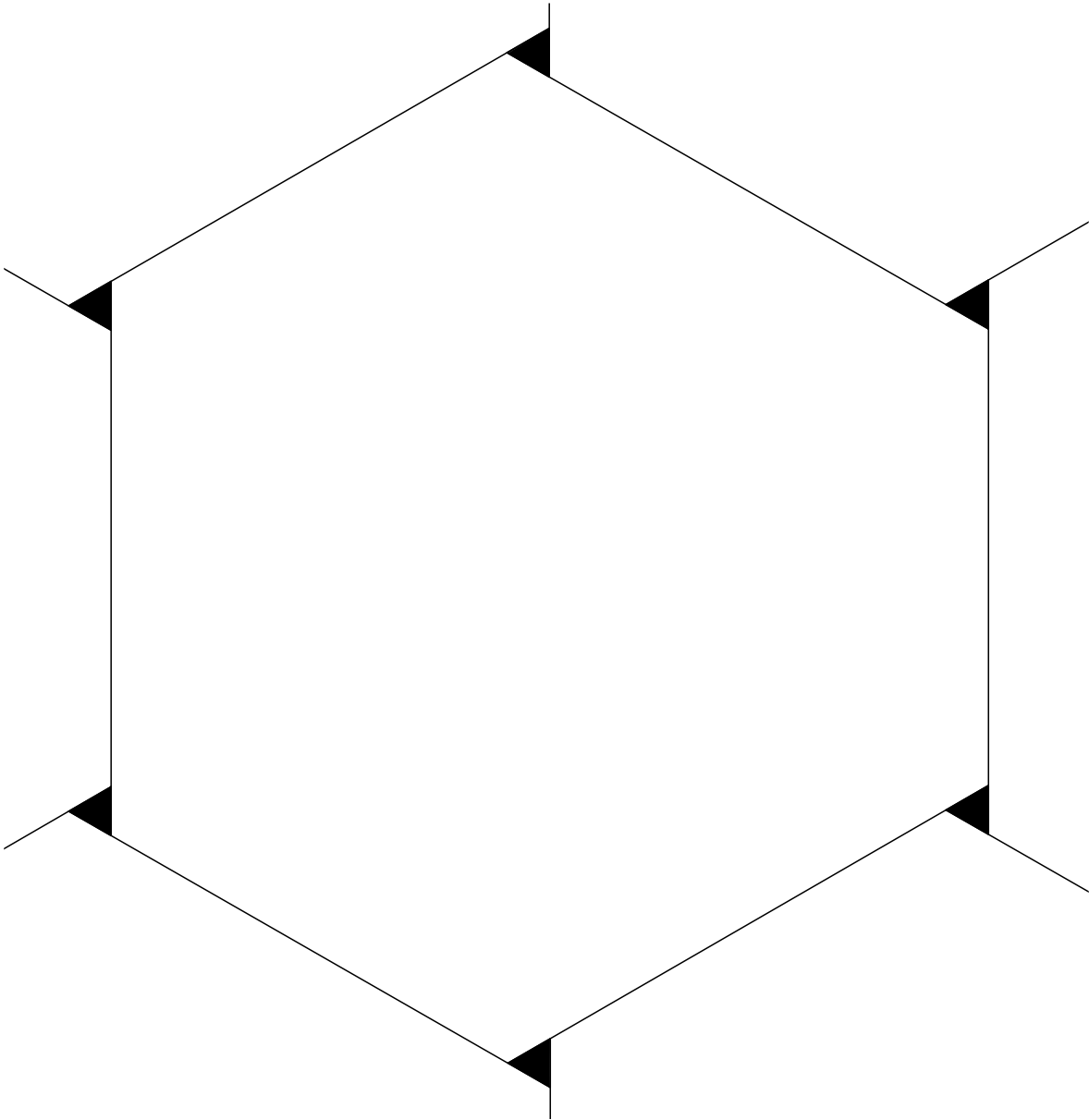


Fig. 21: Part of whole structure with triangular node

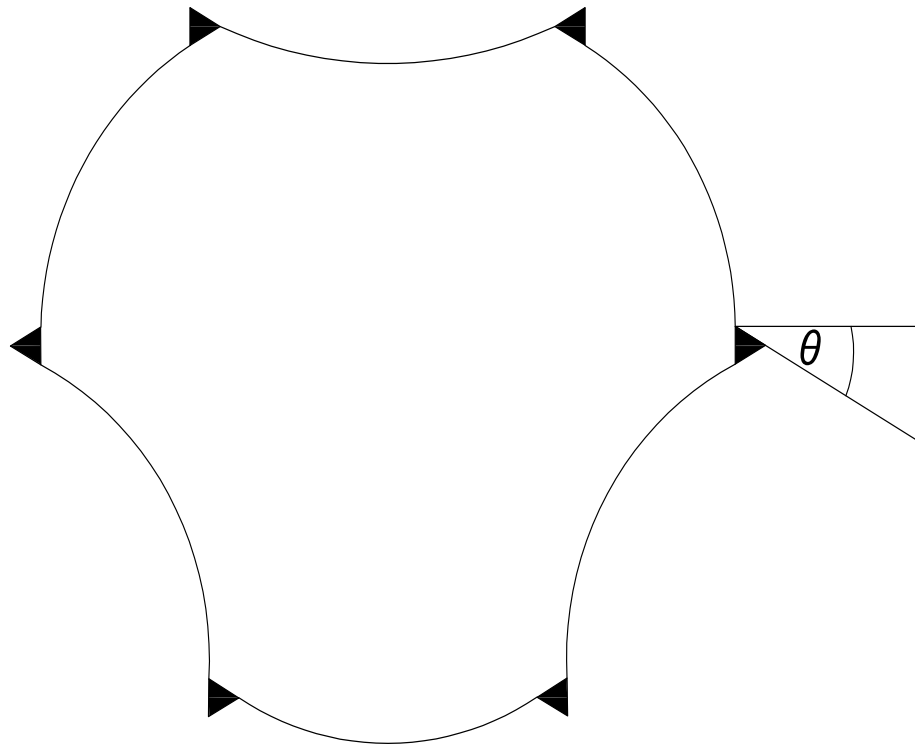


Fig. 22: Deformed diagram of unit cell with triangular node

Considering the geometry of the nodes as triangular and dimension of all sides are H and the length of the bimetallic strip as L , the equation has been formulated. Also, the thermal expansion coefficient of the strip denoted as α_s and the thermal coefficient of the node denoted as α_n .

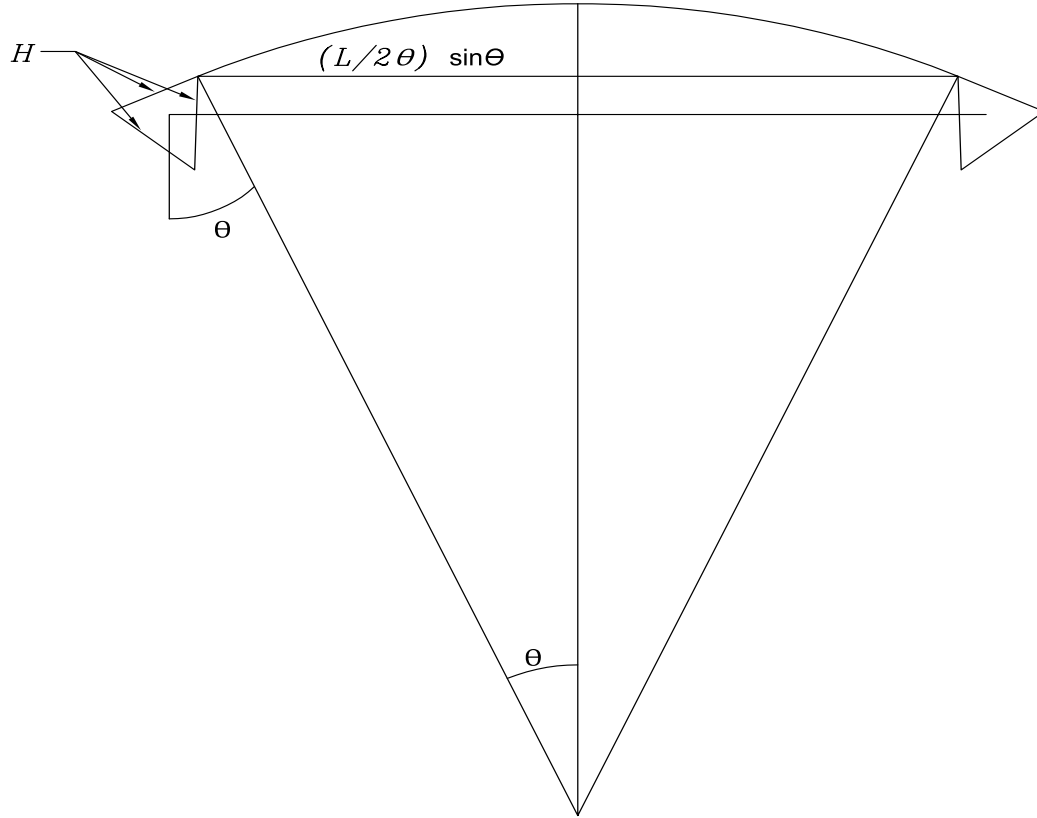


Fig. 23: one strip with two nodes

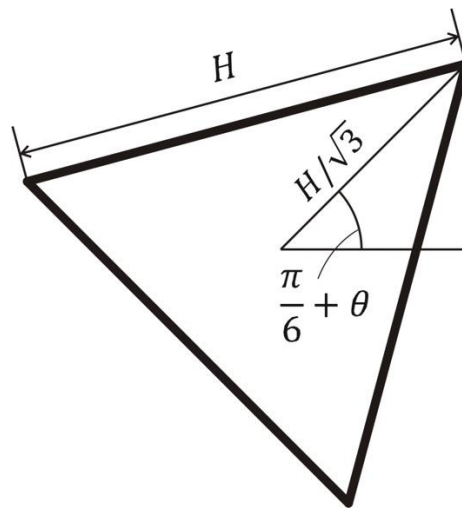


Fig. 24: Triangular node expanded

The deformed length of the strip depends on the curvature and the rate of thermal expansion. Using geometrical theories, the expression can be written as:

$$l = \frac{L_t}{\theta} \sin \theta + \frac{2}{\sqrt{3}} H_t \sin\left[\frac{\pi}{3} - \theta\right] \quad (38)$$

Where, l = deformed length between nodes, L_t = changed length of the strip after temperature has been applied, H_t = changed cross-sectional dimension after temperature has been applied, θ = radius of curvature.

In order to check the validity of the equation, the following condition can be made.

If $T=0$, there will not be any thermal expansion of the strips and nodes and any kind of curvature of the structure as well. Now, from equation (35),

$$l = L + H \quad (39)$$

As temperature is not applied, the dimensions of the strips and the nodes will not be changed. That's why the notations L and H has been used instead of L_t and H_t .

The basic expression for thermally expanded bar is [31]:

$$l_f = l_0 + l_0 \alpha \Delta T \quad (6)$$

Where, l_f = expanded final length, l_0 = initial length, α = thermal expansion coefficient and ΔT = temperature difference.

So, L_t and H_t can be written as:

$$L_t = L(1 + \alpha_s T) \quad (7)$$

$$H_t = H(1 + \alpha_n T) \quad (8)$$

Now, replacing these two terms in equation (2) and rewriting the simplified form of it:

$$l = H(1 + \alpha_n T) \cos \theta + \left(-\frac{H(1 + \alpha_n T)}{\sqrt{3}} + \frac{L(1 + \alpha_s T)}{\theta}\right) \sin \theta \quad (40)$$

This equation has dimension. For further analysis and plotting, it should be dimensionless. To dimensionalize the system, divide by L . So, the dimensionless deformed length between two nodes will be:

$$l(\theta) = h(1 + \alpha_n T) \cos \theta + \left(-\frac{h(1+\alpha_n T)}{\sqrt{3}} + \frac{(1+\alpha_s T)}{\theta}\right) \sin \theta \quad (41)$$

Where, $h = \frac{H}{L}$.

The thermal strain of the system will be:

$$\epsilon_T = \frac{l(\theta, T)}{1+h} - 1 \quad (42)$$

The simplified equation will be:

$$\epsilon_T = -1 + \frac{h(1+\alpha_n T) \cos \theta + \left(-\frac{h(1+\alpha_n T)}{\sqrt{3}} + \frac{1+\alpha_s T}{\theta}\right) \sin \theta}{1+h} \quad (43)$$

The plot of ϵ_T vs T would be:

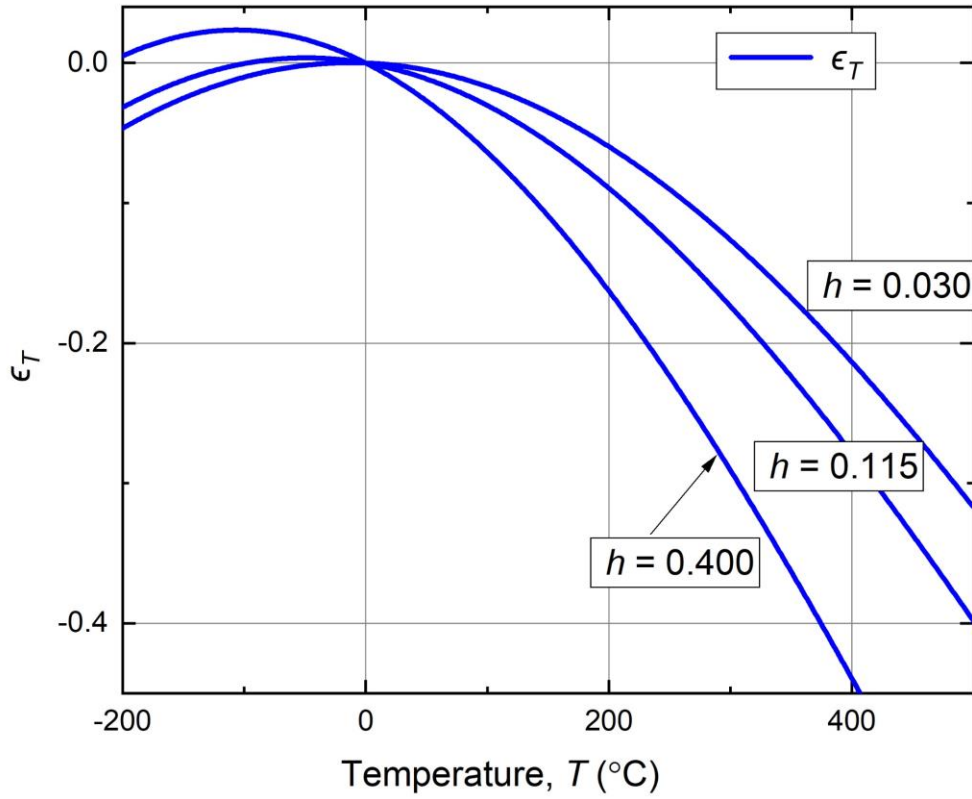


Fig. 25: Using equation (43), thermal strain (ϵ_T) vs temperature (T) has been plotted for three different size ratios ($h = \frac{H}{L}$)

The slope of thermal expansion curve, i.e., the thermal expansion co-efficient is:

$$\alpha_T = \frac{\theta(-3-3hT\alpha_n-3T\alpha_s+\sqrt{3}h\theta+\sqrt{3}hT\alpha_n\theta)\cos\theta+(3+h\theta(3\theta+T\alpha_n(\sqrt{3}+3\theta)))\sin\theta}{3(1+h)T\theta} \quad (44)$$

If $\alpha_s = 0$ and $\alpha_n = 0$, α_T will be:

$$\alpha_T = \frac{\theta(-3+\sqrt{3}h\theta)\cos\theta+(3+3h\theta^2)\sin\theta}{3(1+h)T\theta} \quad (45)$$

$$\theta = \frac{L}{\rho} \quad (15)$$

$$\frac{1}{\rho} = aT \quad (16)$$

“ a ” is a parameter of the strip, which depends on the properties of the strip. The value of “ a ” has to be calculated depending on the bending it shows with the temperature. For this validation, we have used equation (15) & (16) and calculated the value of “ a ” for the bimetallic strip used. To validate the equation experimentally, 60° bending of the 6" strip at $\Delta T = 70^\circ\text{C}$ is assumed. For this assumption, the angle of rotation looks reasonable.

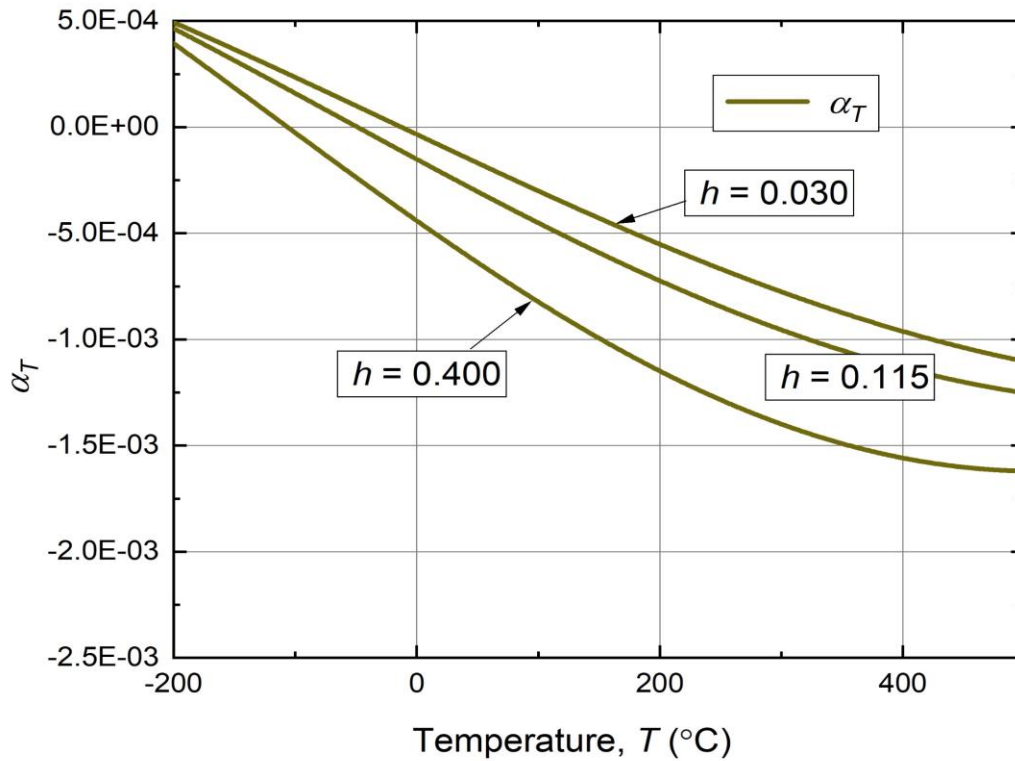


Fig. 26: Thermal expansion coefficient (α_T) vs temperature (T) plot using equation (44) for three different size ratios ($h = \frac{H}{L}$)

Now to know the acceleration of thermal expansion, the thermal strain ϵ should be derivated twice. So, it is as follows:

$$\alpha'_T = \frac{d\alpha}{dT} = \frac{d^2\epsilon}{dT^2} \quad (46)$$

Which can be expressed as:

$$\alpha'_T = \left(\frac{1}{3(1+h)T^2\theta} \left(-\theta \left(6 + h\theta(2\sqrt{3}T\alpha n + 3\theta + 3T\alpha n\theta) \right) \cos[\theta] \right) + (6 - 3(1 + T(2h\alpha n + \alpha s))\theta^2 + \sqrt{3}h(1 + T\alpha n)\theta^3) \sin[\theta] \right) \quad (47)$$

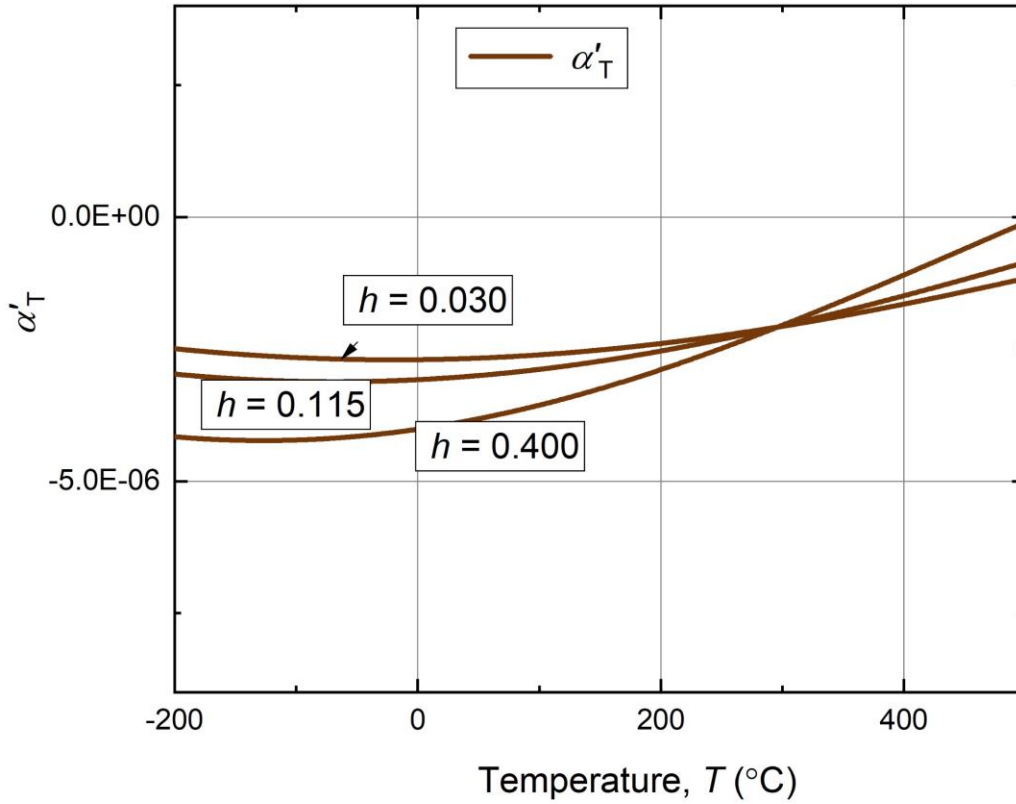


Fig. 27: Acceleration of thermal expansion coefficient (α'_T) vs temperature (T) plot using equation (47) for three different size ratios ($h = \frac{H}{L}$)

N.B.: The above contour map has vertical axis as “ aL ”, which have a dimensionality of $[T]^{-1}$. As the dimension of “ a ” is $[L]^{-1}[T]^{-1}$ and thermal expansion ε has no dimensionality. So, it can be called as the rate of thermal expansion.

$$\alpha'_0 = \lim_{T \rightarrow 0} \alpha'_T = -\frac{aL(aL+3aLh+12h\alpha_n)}{12(1+h)} \quad (48)$$

Where, θ has been replaced by $\theta = \frac{aLT}{2}$

Again,
$$\lim_{h \rightarrow 0} \alpha_0 = -\frac{aL^2}{12}$$

And
$$\lim_{h \rightarrow \infty} \alpha_0 = -\frac{1}{4}aL(aL + \alpha_n)$$

This curve proves that $\frac{d\alpha}{dT}$ at $T = 0$ is a monotonous function in spite of 3 parameters. So that it does not have any maximum in the range.

Comparing the three parameters in a single plot for the size factor of the design shown in the beginning of the chapter, it would present like:

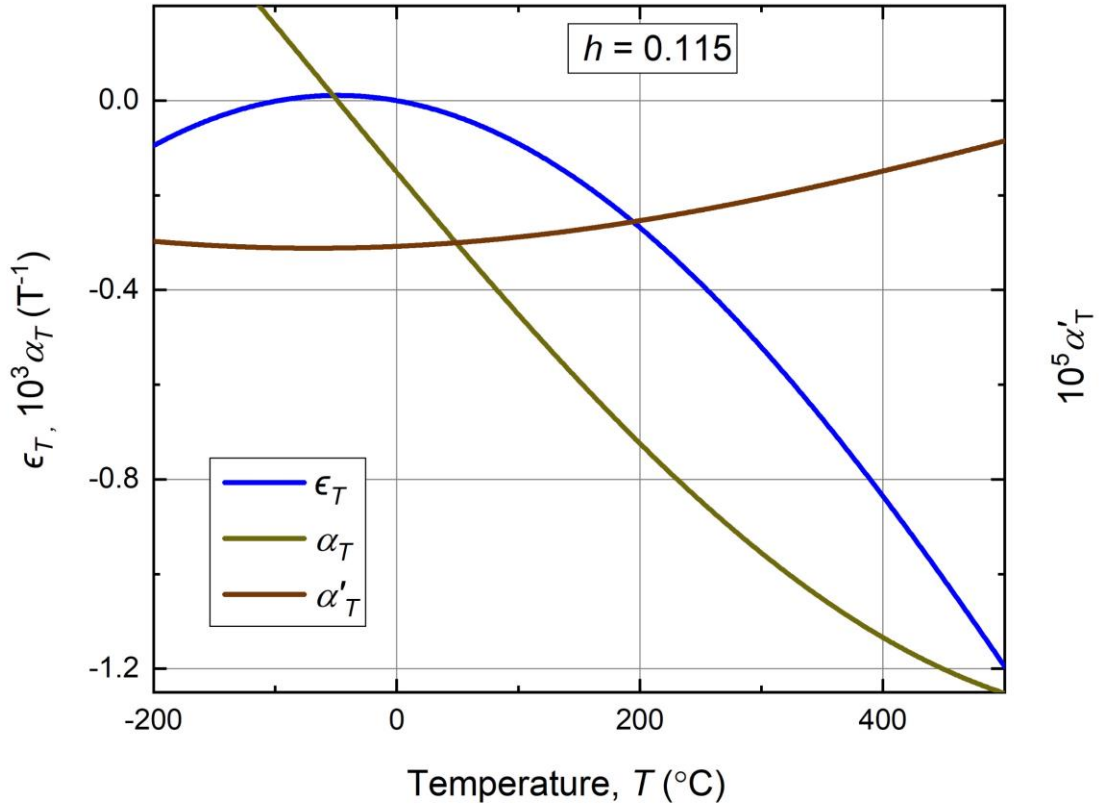


Fig. 28: For size ratio, $h = 0.115$, the three parameters are plotted together. To match the scale, with ϵ_T , α_T and α'_T has been multiplied by 10^3 and 10^5 respectively

To plot α_T and α'_T with ϵ_T , α_T and α'_T should be rescaled. Because these two have very small scale comparatively with ϵ_T . The previous individual graphs have been shown on the original scale.

Considered $\alpha_s = \alpha_n$,

$$\alpha_0 = -\frac{\sqrt{3}aLh}{6(1+h)} + \alpha_s \quad (49)$$

If the points plotted in a contour plot, it would be:

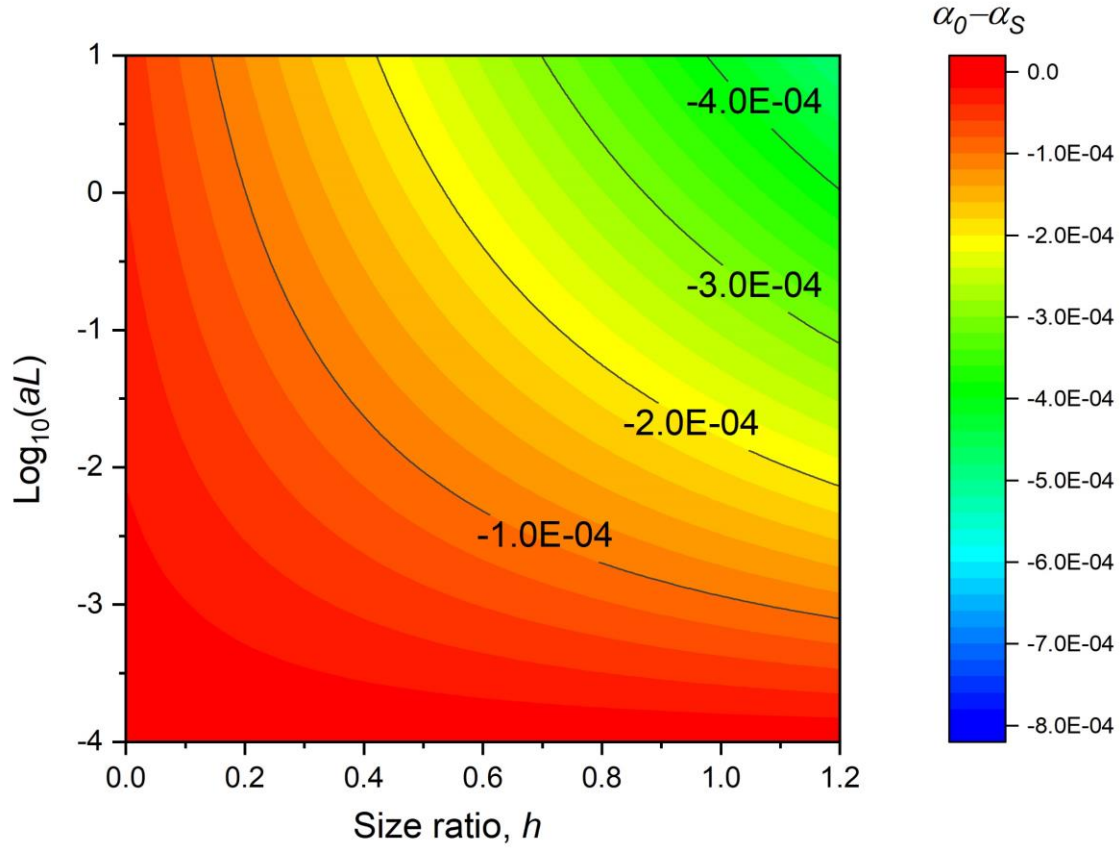


Fig. 29: The contour map has vertical axis as “ $\log_{10} aL$ ”, where “ aL ” have dimensionality of $[T]^{-1}$. As the dimension of “ a ” is $[L]^{-1}[T]^{-1}$ and “ L ” has dimension of $[L]$ (from equation (49)).

So, it can be called as the rate of thermal expansion.

3 Summary and Conclusion

The basic concepts of meta-materials are to design existing materials, such that it will exhibit new properties which is not available on mother materials. This generally is done by engineering and designing the materials. For this case, the materials have been engineered such that it shows thermal bistability and negative thermal expansion. If the dimensions of the nodes have been changed, the properties will change as well (consult the theory above). The node size and the length of the bar are the main parameter here. If these two will change, the behaviors of the model will change as well. Thus, definitely it can be stated that this model is a meta-material design and it will act on temperature.

Throughout the theory, it has been observed that for all three cases, thermal expansion coefficient (α_T) is monotonously linear. For the circular node, α_T is not always decreasing. After certain temperature, i.e., 295°C, which is also critical temperature of this design, α_T starts to increase. It will still remain negative, but it will no longer be monotonously decreasing. If we design geometrically this design with circular node such a way that after the strips will touch each other, they will still move away, we can achieve positive α_T .

The contour plots are one of the most important plots for this study. All three have been plotted with $\log_{10} aL$ vs size ratio (h). Whereas size ratio ($h = \frac{H}{L}$) and the Y-axis can be interpreted as $(\alpha_0 - \alpha_s)$. α_0 is the coefficient at $T = 0$ and α_s is the thermal expansion coefficient of the strip.

The thermal expansion coefficient expressions for different node designs at $T = 0^\circ\text{C}$ are:

- For square node:

$$\alpha_0 = \frac{-aLh}{2(1+h)} + \alpha_s$$

- For circular node:

$$\alpha_0 = -\frac{aLd}{2} + \alpha_s$$

- For triangular node:

$$\alpha_0 = \frac{-\sqrt{3} aLh}{6(1+h)} + \alpha_s$$

So, at $h = 0.115$, $L = 0.064$, $a = 0.15$ and $T = 0$, the values will be as follows:

Table 1: Comparison of α_T and α'_T between three node types

	Square Node	Circular Node	Triangular Node
α_T	$-4.951E - 4$	$-5.52E - 4$	$-2.86E - 4$
α'_T	$-9.26E - 6$	$-5.12E - 5$	$-9.26E - 6$

Comparing the above table, the value of thermal expansion coefficient for triangular node is almost half of the value of the square node. But the value for circular node is higher among them. For the acceleration rate of thermal expansion coefficient, the values are same for both square and triangular node. But the value for circular node is much higher than others.

So, for the practical use, circular node is definitely better than other two.

4 Future Work

Throughout the text, we have discussed about thermal strain (ϵ_T), thermal expansion coefficient (α_T) and acceleration rate of thermal expansion coefficient (α'_T). All the values have been used in the text is theoretical. No experimental work has been done to measure them. So, for further work, the values of α_T and α'_T can be measured experimentally.

Solving the critical angle of the structure with triangular node is comparatively difficult than the square node and circular node structures. As it has six sides, when they bend due to temperature applied, it's hard for them to touch each other. Theoretically, it has ended up with a very complex equation with both $\tan \theta$ and $\sec \theta$ in it. So, it is quite impossible to find the critical value of θ , i.e., the angle of rotation. Hence, it's not possible to find out the critical temperature of the structure with triangular node. So, this is the something which can be worked on further. This thesis is based on theoretical calculations and derivations. For future work, the practical models can be made and tested to observe same properties. For theoretical purpose, I would like to do the same numerical method in the equation derived from the curvature of the strips.

Thermomechanical Metamaterials are comparatively new field of study. There have been a lot about these metamaterials to be discovered. We are trying to design and develop theory of snapping thermomechanical metamaterials.

I have also designed few non-local lattice structures and printed it using polymer. Based on that we are also trying to develop non-reversible thermomechanical metamaterials.

Metal 3D printing is also a field we are interested in. Printing bimetallic material is difficult till now. We planned to work on that field and try to come up with the solution for this problem.

And at last, as an engineer, we are also trying to make everything very efficient specially for 3D printing. The models which we are going to design, we will try to make those very efficient and quick to respond.

5 References

- [1] Veselago, V.G.; The electrodynamics of substances with simultaneously negative values of permittivity and permeability. *Soviet Physics Uspekhi* **1968**, *10*, 509–51
- [2] Smith, D.R.; Padilla, W.J.; Vier, D.C.; Nemat-Nasser, S.C.; Schultz, S.; Composite medium with simultaneously negative permeability and permittivity. *Physical Review Letter* **2000**, *84*, 4184–4187.
- [3] Pendry, J.B.; Holden, A.J.; Stewart, W.J.; Youngs, I.; Extremely low frequency plasmons in metallic mesostructures. *Physical Review Letter* **1996**, *76*, 4773–4776.
- [4] Pendry, J.B.; Holden, A.J.; Robbins, D.J.; Stewart, W.J.; Magnetism from conductors and enhanced nonlinear phenomena. *IEEE Trans. Microwave Theory Technology* **1999**, *47*, 2075–2084.
- [5] Pendry, J.B.; Negative refraction makes a perfect lens. *Physical Review Letter* **2000**, *85*, 3966–3969.
- [6] Soukoulis, C.; Wegener, M.; Past achievements and future challenges in the development of three-dimensional photonic metamaterials. *Nature Photonics* **2011**, *5*, 523–530.
- [7] Zhou, J.; Koschny, T.; Kafesaki, M.; Economou, E.N.; Pendry, J.B.; Soukoulis, C.M.; Saturation of magnetic response of split-ring resonators at optical frequencies. *Physical Review Letter* **2005**, *95*, 223902.
- [8] Miyamaru, F.; Saito, Y.; Takeda, M.W.; Hou, B.; Liu, L.; Wen, W.; Sheng, P.; Terahertz electric response of fractal metamaterial structures. *Physical Review Letter B* **2008**, *77*, 045124.
- [9] Guariglia, E.; Entropy and Fractal Antennas. *Entropy* **2016**, *18*, 84.
- [10] Walser, R. M.; Electromagnetic Metamaterials. *SPIE. The international society for optics and phonetics* **2001**, 4467.
- [11] Cummer, S.A.; Christensen, J.; Alu, A. Controlling sound with acoustic metamaterials. *Nature Review Materials* **2016**, *1*, 16001.
- [12] Hussein, M.I.; Leamy, M.J.; Ruzzene, M. Dynamics of phononic materials and structures: Historical origins, recent progress, and future outlook. *Applied Mechanics Reviews* **2014**, *66*.
- [13] Lui, Z.; Zhang, X.; Mao, Y.; Zhu, Y.; Yang, Z.; Chan, C.; Sheng, P. Locally resonant sonic materials. *Science* **2000**, *289*.

- [14] Wang, Y.Z.; Li, F.M.; Huang, W.-H.; Jiang, X.; Wang, Y.-S.; Kishimoto, K. Wave band gaps in two-dimensional piezoelectric/piezomagnetic phononic crystals. *International Journal of Solids and Structures* **2008**, *45*, 4203–4210.
- [15] Yu, X.L.; Zhou, J.; Liang H.Y.; Jiang, Z.Y.; Wu, L.L.; Mechanical metamaterials associated with stiffness, rigidity and compressibility: A brief review. *Progress in Materials Science* **2018**, *94*, 114–173.
- [16] Bertoldi, K.; Vitelli, V.; Christensen, J.; van Hecke, M. Flexible Mechanical Metamaterials. *Nature Review Materials* **2017**, *2*(11), p. 17066.
- [17] Kolpakov A.G.; On the determination of the averaged moduli of elastic gridworks. *Prikl. Material Mekh.* **1985**, *59*, 969–977.
- [18] Lakes, R.S.; Foam structures with a negative Poisson's ratio. *Science*. **1987**, *235*, 1038–1040.
- [19] Lakes, R.S.; Negative Poisson's ratio materials. *Science*. **1987**, *238*, 551.
- [20] Kaminakis, N.T.; Stavroulakis, G.E. Topology optimization for compliant mechanisms, using evolutionary- hybrid algorithms and application to the design of auxetic material. *Composites Part B: Engineering*, **2012**, *43* (6): 2655–2668
- [21] Stavroulakis, G.E.; Auxetic behaviour: Appearance and engineering applications. *Physica Status Solidi B*. **2005**, *242* (3): 710–720.
- [22] Dong, L.; Lakes, R.; Advanced damper with high stiffness and high hysteresis damping based on negative structural stiffness. *International Journal of Solids and Structures* **2013**, *50*, 2416–2423.
- [23] Spitas, V.; Spitas, C.; Michelis, P. Modeling of the elastic damping response of a carbon nanotube–polymer nanocomposite in the stress–strain domain using an elastic energy release approach based on stick–slip. *Mechanics of Advanced Materials and Structure* **2013**, *20*, 791–800.
- [24] Craciun G.; Tang Y.; Feinberg, M.; Understanding bistability in complex enzyme-driven reaction networks. *The National Academy of Sciences* **2006**, *103* (23), 8697–8702.
- [25] Nicolau, Z. G.; Motter, A. E. Mechanical metamaterials with negative compressibility transitions, *Nature Materials* **2012**, *11*, 608.

- [26] Nicolau, Z. G.; Motter, A. E.; Longitudinal inverted compressibility in super-strained metamaterials, *Journal of Statistical Physics* **2013**, *151*, 1162.
- [27] Chen, M. L.; Karpov E. G.; Bistability and thermal coupling in elastic metamaterials with negative compressibility, *Physical Review E*. **2014**, *90*, 033201.
- [28] Imre, A.R.; Metamaterials with negative compressibility – a novel concept with a long history, *Materials Science-Poland*. **2014**, *32*, 126–129.
- [29] Karpov, E.G.; Danso, L.A.; Klein, J.T.; Negative extensibility metamaterials: Occurrence and design-space topology. *Physical Review* **2017**, *96*.
- [30] Sophia, R Sklan; Baowen, Li; Thermal metamaterials: functions and prospects, *National Science Review*, *Volume 5, Issue 2*, **2018**, 138–141.
- [31] Timoshenko, S.P.; *Journal of the Optical Society of America* **1925**, *11*, 233.
- [32] https://en.wikipedia.org/wiki/Thermal_expansion

VITA

NAME: Debajyoti Saha

EDUCATION: B.Tech., West Bengal University of Technology, West Bengal, India, 2017
M.S., University of Illinois at Chicago, Chicago, Illinois, 2019

HONORS: Chancellor's Student Service Award, University of Illinois at Chicago, April 2018

MEMBERSHIP: Structural Engineering Association of Illinois (Student)
American Institute of Steel Construction (Student)

EXPERIENCE: Summer Intern at KCS Corporation, Schaumburg, Illinois, 2018
Summer Intern at UNITECH Uniworld, Kolkata, West Bengal, India, 2016